The Effect of Patulin on Oxidative Stress and Global DNA Methylation in C57BL/6 Mice Hearts

by

NOXOLO L. RADEBE

BSc. B. Med. Sc (Hons) (UKZN)

Submitted in fulfilment of the requirements for the degree of Master of Medical Science

Discipline of Medical Biochemistry

School of Laboratory Medicine and Medical Sciences

College of Health Sciences

University of KwaZulu-Natal

2024

DECLARATION

I, Radebe Noxolo Laurah, Student Number**:** 218027949 declare that:

i. The research reported in this dissertation, except where otherwise indicated, is my original work.

ii. This dissertation has not been submitted for any degree or examination at any other university.

iii. This dissertation does not contain other person's data, pictures, graphs or other information, unless specifically acknowledged as being sourced from other persons.

iv. This dissertation does not contain other person's writing, unless specifically acknowledged as being sourced from other researchers. Where other written sources have been quoted then:

   a. Their words have been re-written, but the general information attributed to them has been referenced.

   b. Where their exact words have been used, their writing has been placed inside quotation marks and referenced.

v. Where I have reproduced a publication of which I am an author, co-author or editor, I have indicated in detail which part of the publication was written by myself alone and have fully referenced such publications.

vi. This dissertation does not contain text, graphics or tables copied and pasted from the internet, unless specifically acknowledged, and the source being in the dissertation and the reference sections.

Student Signed: NL Radebe **Date:** 20/11/2024

ACKNOWLEDGMENTS

Dr T. Ghazi

Thank you for believing in me, motivating me, and providing me with the best supervision any student could wish for. Thank you so much for your advice, care and extended love, I appreciate it all.

Professor A.A. Chuturgoon

Thank you for your supervision, guidance, and support.

Family and Friends

Thank you so much for your financial and emotional support.

College of Health Sciences

I appreciate the funding received.

PRESENTATIONS

1. **Investigating oxidative and epigenetic alterations of patulin in C57BL/6 mice hearts** **Radebe N**, Chuturgoon AA, Ghazi T

   College of Health Sciences Research Symposium (27th – 28th August 2024), University of KwaZulu-Natal, Durban, South Africa. Oral presentation.

2. **Investigating oxidative and epigenetic alterations of patulin in C57BL/6 mice hearts** **Radebe N**, Chuturgoon AA, Ghazi T

   School of Laboratory Medicine and Medical Sciences Research Day (27th September 2024), University of KwaZulu-Natal, Durban, South Africa. Poster presentation.

TABLE OF CONTENTS

LIST OF FIGURES

LIST OF TABLES

ABBREVIATIONS

AA	Amino acid
APS	Ammonium persulfate
ARE	antioxidant response element
BCA	Bicinchoninic acid
BSA	Bovine serum albumin
CAT	Catalase
cDNA	Complementary DNA
DNA	Deoxyribonucleic acid
DNMT	DNA methyltransferase
dNTP	Deoxynucleotide triphosphate
ELISA	Enzyme-linked immunosorbent assay
FAO	Food and Agriculture Organization
Gpx	Glutathione peroxidase
HIV	Human immunodeficiency virus
H_2O_2	Hydrogen peroxide
HRP	Horseradish peroxidase
Keap1	Kelch-like ECH-associated protein 1
MBD2	Methyl-CpG binding domain 2
MDA	Malondialdehyde
NaCl	Sodium chloride
Nrf2	Nuclear factor erythroid 2-related factor 2
OH^-	Hydroxide ion
OS	Oxidative stress
PAT	Patulin
PBS	Phosphate-buffered saline

PCR	Polymerase chain reaction
qPCR	Quantitative PCR
ROS	Reactive oxygen species
RT	Room temperature
SA	South Africa
SDS	Sodium dodecyl sulphate
SDS-PAGE	Sodium dodecyl sulphate-polyacrylamide gel electrophoresis
SOD2	Superoxide dismutase 2
TBA	Thiobarbituric acid
TBARS	Thiobarbituric acid reactive substances
TEMED	N,N,N′,N′-tetramethylenediamine
Tris	Tris (hydroxymethyl) aminomethane
TTBS	Tris-buffered saline with Tween 20
USA	United States of America

ABSTRACT

Mycotoxins are chemical compounds produced by fungi that, when ingested, induce a variety of diseases including hepatotoxicity, nephrotoxicity, gastrointestinal toxicity, neurotoxicity, and immunotoxicity. Patulin (PAT) is a common mycotoxin produced by *Penicillium*, *Aspergillus*, and *Byssochlamys* fungal species, and is commonly found in apples and its products. Researchers have reported that consumption of PAT-contaminated foods causes nephrotoxicity and hepatotoxicity; however, its effects on the heart are unknown. Following reports that PAT causes oxidative stress and epigenetic changes, this study assessed if PAT induces oxidative stress and global DNA methylation in C57BL/6 mice hearts. Methods included: (i) ten mice treatment with PAT (2,5mg/kg) and PBS (0,1M) for 24hr, five mice per treatment group, (ii) thiobarbturic acid reactive substances (TBARS) assay (lipid peroxidation), (iii) quantitative polymerase chain reaction (gene expression of kelch-like ECH-associated protein 1 (Keap1), nuclear factor erythroid 2-related factor 2 (Nrf2), glutathione peroxidase (GPx), superoxide dismutase 2 (SOD2), catalase (CAT), methyl-CpG binding domain protein 2 (MBD2), DNA methyltransferases (DNMT1, DNMT3A, DNMT3B), (iv) western blot (protein expression of Nrf2, SOD2, CAT, MBD2, DNMT3A and DNMT1), (v) enzyme-linked immunosorbent assay (global DNA methylation levels). PAT caused an induction of oxidative stress as indicated by the significant increase in malondialdehyde (MDA) levels (0.52-fold, p = 0.005). PAT significantly increased gene expression of *Nrf2* (1.20-fold, p=0.049), *GPx* (1.20-fold, p = 0.028), *SOD2* (1.40-fold, p = 0.042) and *CAT* (0.90-fold, p = 0.038); and significantly decreased gene expression of *keap1* (1.10-fold, p = 0.007). PAT increased expression of Nrf2 protein, significantly (0.64-fold, p = 0.005), SOD2 (2.40-fold, p = 0.020), and CAT (1.88-fold, p = 0.004). Additionally, PAT suppressed the gene expression of *DNMT3A* (0.41-fold, p = 0,0001) and *MBD2* (0.45-fold, p = 0,0001) and increased the gene expression of *DNMT1* (1.48-fold, p = 0,02) and *DNMT3B* (1.62-fold, p = 0,04). PAT increased the protein expression of DNMT1 (0.68-fold, p=0.029); and significantly decreased the protein expression of MBD2 (0.48-fold, p=0.008) and DNMT3A (0.50-fold, p = 0.0001). The alterations in DNMTs and MBD2 led to PAT-induced global DNA hypermethylation (1.72-fold, p = 0,02). In conclusion, PAT induced oxidative stress and global DNA hypermethylation in C57BL/6 mice hearts and is toxic to the heart.

Keywords: Patulin, oxidative stress, global DNA methylation, C57BL/6 mice heart, mycotoxin

CHAPTER 1: INTRODUCTION

The Food and Agriculture Organization (FAO) declared mycotoxin contamination of foods as a global issue with an estimated 25% in crops, an integral source of nutrition (Luo *et al*., 2021, He, 2011). This poses a threat to agriculture, the economy, health, and food security (Eskola *et al*., 2020). In areas such as South Africa, this issue is common as these areas are still developing and are often poverty-stricken and have malnutrition as an integral concern, thus consuming food that is contaminated with mycotoxin is an ultimatum (Stoev, 2024). New agricultural practices and rapid governmental screening have been implemented in the past years to reduce mycotoxin contamination; however, this issue has persisted. Hence, mycotoxin contamination is considered a recurring issue (Truong *et al*., 2023).

. The potency, carcinogenicity, toxicity, and lethality of mycotoxins that are ingested by animals and humans demand proper attention to evaluate the levels of it contained in various foods that are commonly consumed (Awuchi *et al*., 2020). The most studied mycotoxins include aflatoxins, ochratoxin, zearalenone, fumonisins, trichothecenes and patulin. Transmission of these mycotoxins to humans is commonly through eating meat from animals that were fed contaminated diets or ingestion of spices while processing animal products (El-Sayed *et al*., 2022). Mycotoxins generally have a very low molecular weight of less than 1000 Da, which enables them to be unavoidable. Mycotoxicosis is a term used to define diseases caused by mycotoxins (Janik *et al*., 2020).

Patulin (PAT) is a mycotoxin produced by a cluster of fungi mainly in vegetables and fruits, especially apples, grapes, and dry maize (Awuchi *et al*., 2022). A study showed that in an area of approximately 800 000 hectares of cultivated fruits (11% are apples and 2% are grapes), where 7.05 million tons of the production, 1% is grapes and 8% is apples that were contaminated with PAT (Hussain *et al*., 2020). This accentuates a decline in agricultural production and may lead to serious economic risk. Moreover, the consumption of PAT-contaminated foods poses a serious health risk to humans and animals. It causes toxicities to the nervous system, immune system, and skin, leading to damage to organs, including the kidneys, liver and heart (Zhang *et al*., 2022b). It has a precursor known as 6-methyl salicylic acid that forms a part of derivatives of acetyl-CoA, both of which are polyketides and possible carcinogens. These derivatives can cause gene mutations (Awuchi *et al*., 2022).The heart is a vital organ with specialized protective tissues. It is one of the organs that are usually vulnerable to PAT toxicity when consumed because it regulates the body's circulation. Previous studies have shown how cardiotoxicity can be a threat to human life, causing death at times (Zhang *et al*., 2022a). Research on PAT-induced cardiotoxicity is currently limited; however, studies on the kidney and liver suggested that PAT caused oxidative stress by depleting antioxidants (Pillay *et al*., 2020), and can alter epigenetics (Mazibuko *et al*., 2024).

Oxidative stress is a relative generation of excessive reactive oxygen species (ROS) over antioxidants. This leads to serious health issues such as cardiovascular diseases, neurodegenerative diseases, and

diabetes mellitus, amongst others (Hayes *et al*., 2020). In the heart, the accumulation of ROS above the cellular threshold causes an imbalance in the tissue and leads to cardiac distress. Moreover, cardiac oxidative stress regulates a variety of genes involved in cellular homeostasis, including injury and antioxidant defence (Liu *et al*., 2023b), and dysregulation of this results in organ dysfunction.

Epigenetic modifications refer to inherited gene activity alteration occurring without alterations to the DNA sequence itself (Davalos and Esteller, 2023). It plays an essential role in several biological processes and diseases (Zhao *et al*., 2020). Epigenetics helps us understand the depth and pathways of these modifications. Previously, Liu *et al* found that regulating oxidative stress by targeting epigenetic modifications is a promising therapeutic mechanism to prevent cardiac-related diseases, notably cardiac fibrosis (Liu *et al*., 2023b).

DNA methylation is a common epigenetic process (Lu *et al*., 2020). It primarily takes place at the cytosine residues within CpG dinucleotides and is regulated by DNA methyltransferases (DNMT1, DNMT3A, and DNMT3B) and methyl-CpG-binding domain 2 protein (MBD2) (Mazibuko *et al*., 2024, Sugiyama *et al*., 2021). Research has shown that oxidative stress has been involved in the damage of DNA, this lesion is usually due to the production of hydroxyl radical which rearranges the chromosome, breaks the DNA strand, and modifies and deletes bases. This interference has been shown to disrupt the function of DNA as a substrate for the DNMTs, resulting in hypomethylation (Franco *et al*., 2008). Studies have shown that PAT alters global DNA methylation in C57BL/6 mice kidneys and human embryonic kidney cells (Mazibuko *et al*., 2024, Pillay *et al*., 2021).

1.1. Research questions

- Does PAT induce oxidative stress in C57BL/6 mice hearts?
- Does PAT alter NRF2-antioxidant signaling in C57BL/6 mice hearts?
- Does PAT alter global DNA methylation levels in C57BL/6 mice hearts?
- What is the effect of PAT on DNMT and MBD2 expression levels in C57BL/6 mice hearts?

1.2. The Aim

To determine the effect of patulin on C57BL/6 mice hearts by assessing oxidative stress and global DNA methylation levels.

1.3. Problem statement

Cereals are an important source of food and are the most prone to mycotoxin contamination. This contamination is unavoidable because of the change in climate, which impacts fungal growth and the production of mycotoxins found in crops (Khodaei *et al*., 2021). This global issue calls for

resolutionas it has the potential to negatively impact the economy and food security. Patulin is a problematic food contaminant. Previous studies have revealed that PAT has various toxic effects in organs, tissues, and cells, including the stomach, kidneys, liver, skin, blood and neurons (Fan and Hu, 2024). A study by Zhang *et al*. revealed a rarely reported toxicity of PAT in the heart; this study concluded that PAT induced cardiotoxicity by potentially inducing oxidative stress and apoptosis (Zhang *et al*., 2022a). Another study by Mazibuko *et al*. reported that PAT induced global DNA methylation (Mazibuko *et al*., 2024) in kidney tissues. Therefore, this study evaluated the presence of PAT-induced oxidative stress and global DNA methylation in causing cardiotoxicity in C57BL/6 mice, and the relationship between the two pathways. No data has been reported on PAT causing oxidative stress or DNA methylation in C57BL/6 mice hearts.

1.4. Hypothesis

PAT induces oxidative stress and global DNA hypermethylation in C57BL/6 mice hearts.

1.5. Objectives

- To assess the effect of PAT on oxidative stress by measuring the levels of malondialdehyde (MDA) utilizing the thiobarbituric acid reactive substances (TBARS) assay.
- To investigate how PAT affects oxidative stress and global DNA methylation by evaluating the gene and/or protein expression of oxidative stress regulators (Keap1, Nrf2, SOD2, CAT, and GPx), DNA methyltransferases (DNMT1, DNMT3A and DNMT3B), and DNA demethylase (MBD2) using quantitative polymerase chain reaction (qPCR) and western blotTo assess the effects of PAT on global DNA methylation levels using enzyme-linked immunosorbent assay (ELISA).

CHAPTER 2: LITERATURE REVIEW

2.1. Mycotoxins

Food insecurity is an integral socio-economic issue in third-world economies, notably, in areas that largely depend on maize and its derivatives. Contamination of these crops threatens human life, the country's economy and growth (Mamo *et al*., 2020, Hamad *et al*., 2023). Mycotoxins are mostly found in crops and food of animals, pre- and post-harvesting, under adverse environmental conditions (Yiannikouris and Jouany, 2002b). This calls for a need to implement simple and accessible agricultural practices which will decrease the amount of produce contaminated by mycotoxins (Aristil *et al*., 2020).

Mycotoxins are naturally produced by fungi and are a threat to animal and human health (El-Sayed *et al*., 2022). The most common mycotoxin-producing fungi are *Aspergillus*, *Fusarium and Penicillium (Figure 1)* (Yiannikouris and Jouany, 2002b). Under optimal environmental conditions such as humidity, appropriate temperature and enough nutrients, fungi produce enormous amounts of mycotoxins (Ülger *et al*., 2020). Mycotoxins are produced in cereal grains, maize, fruits and vegetables throughout pre- and post-harvesting processes and during storage (Yiannikouris and Jouany, 2002a). Their very low molecular weight (less than 1000 Da) and their natural mode of production makes them unavoidable (Janik *et al*., 2020). The common studied mycotoxins, out of 400 discovered mycotoxins, are aflatoxins, fumonisins, zearalenone, patulin, ochratoxin and trichothecenes (Janik *et al*., 2020).

Mycotoxins are potentially hazardous compounds which can invade the food chain either directly or indirectly (El-Sayed *et al*., 2022). Since these compounds can contaminate both crops and animal products, it poses a great threat in the food chain (Janik *et al*., 2020). They are classified in accordance with their effects in the human body, notably, tissues as hepatotoxins, nephrotoxins, immunotoxins, and neurotoxins (Ülger *et al*., 2020). Research shows that mycotoxins can also be genotoxic and/or carcinogenic and the severity of their effects relies mainly on the availability of vitamins in the body, energy and status of infectious disease, dose, species susceptibility, duration of intoxication (Furian *et al*., 2022, Ülger *et al*., 2020, Awuchi *et al*., 2020).

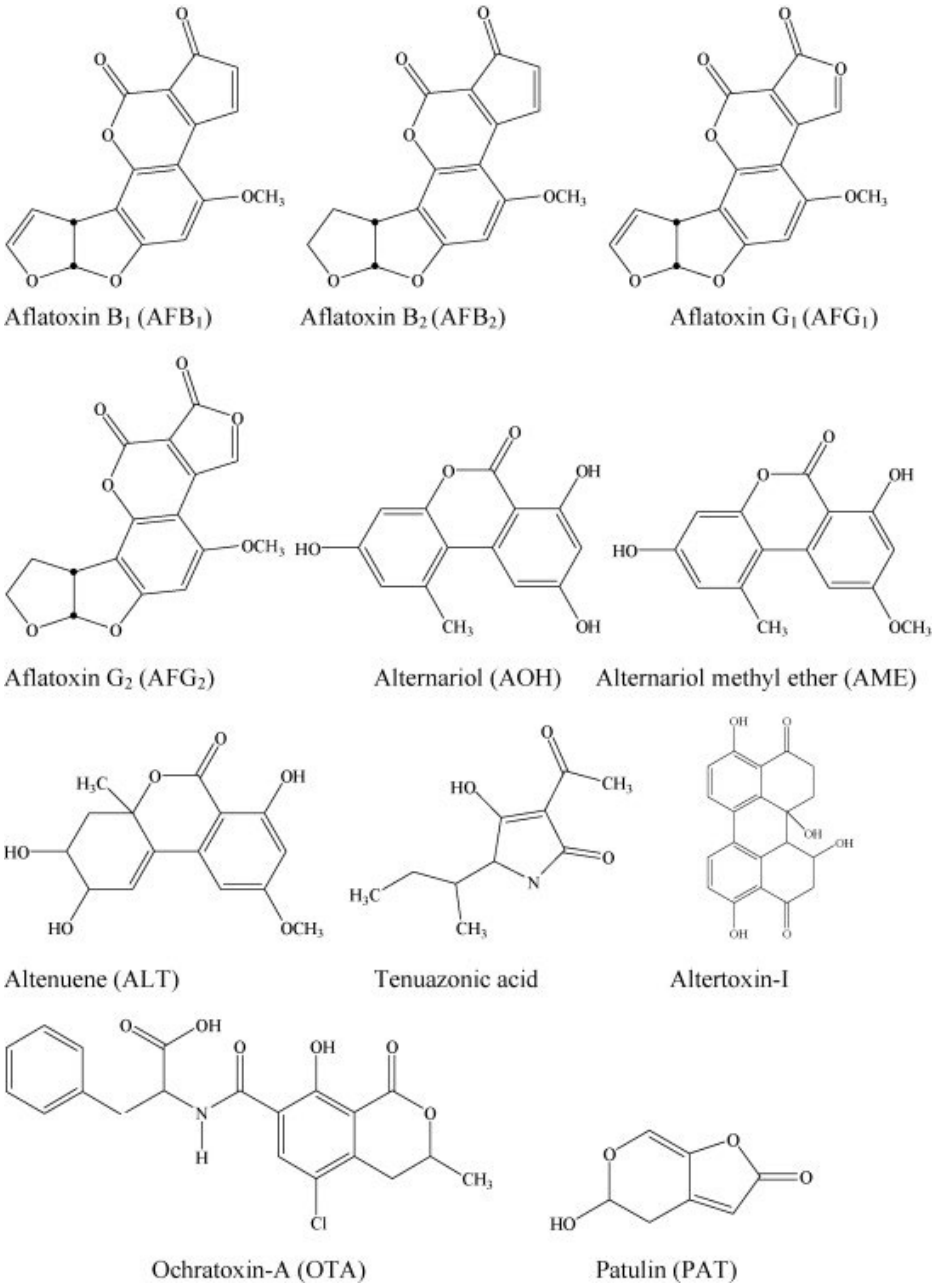

Figure 1**:** Commonly studied mycotoxins (Fernández-Cruz *et al*., 2010).

Although mycotoxins are well known for their negative effects on animals and humans, they also exhibit positive effects under certain conditions. They may be pathogenic against bacteria, and in the presence of human immunodeficiency virus (HIV) or other risk factors of diseases, they become chemotherapeutic or immuno-suppressive drugs (Ülger *et al*., 2020). Some studies have shown that ingestion of mycotoxins reduces the production of both milk and eggs, influences behavioral changes and reduces growth in animals (Furian *et al*., 2022).

Structurally, mycotoxins have diverse chemical structures with no single formula that suits them all. They merely function as a defensive response to the changing environment and in accordance with

nutrient availability. They are sometimes produced as a self-defence response of fungi and exhibit fungal pathogenicity by dissolving cellular membranes (Aristil *et al*., 2020). Although all mycotoxins are produced by fungi, not all toxins produced by fungi are called mycotoxins. This largely depends on the concentration of the toxic compound and its target, for example, the fungal product penicillin is toxic to bacteria but is invaluable to humans as an antibiotic (Klich *et al*., 2003, Awuchi and Ogueke, 2021).

Exposure to mycotoxins results in health issues known as mycotoxicoses (Janik *et al*., 2020). The transmission of these mycotoxins is common through inhalation, ingestion or dermal routes. Consumption of meat, meat products or spices that were contaminated with mycotoxins is the most common mode of mycotoxin exposure in humans (Janik *et al*., 2020, El-Sayed *et al*., 2022). South Africa (SA) is one of the countries frequently affected by mycotoxin contamination because malnourishment is a common issue and cereal grains form a huge part of the staple diet (Klich *et al*., 2003). Mycotoxin contamination is further exacerbated where food handling and storage are poorly conducted (Janik *et al*., 2020).

Table 1: Mycotoxins, the fungal genus producing it, major contaminating foods and associated mycotoxicoses (El-Sayed *et al*., 2022)

Mycotoxin	**Genus**	**Major food**	**Mycotoxicoses & toxic effects**
Aflatoxin	*Penicillium* *Aspergillus*	Cereals, feeds, oilseeds, pulp, coconut	Hepatotoxicity, carcinogenicity, suppression of immune system, DNA structure alteration, renal lesions, hepatitis
Fumonisin	*Fusarium*	Cereals, corn	Pulmonary oedema, neurotoxicity, carcinogenicity, liver damage, heart failure, oesophageal cancer
Patulin	*Aspergillus* *Penicillium* *Byssochlamys*	Apples, grapes, peaches, wheat, pears, olives, cereals, silage, feeds	Skin lesions, brain haemorrhage, neural disorders, antibacterial impact, lung, skin cancer, mutagenicity

Zearalenone	*Fusarium*	Cereals, corn, silage, fodder, timothy grass	Carcinogenic, hormonal imbalance oestrogen effect, reproductive problems, teratogenic

Mycotoxin management and reduction in produce have been attempted; however, its production has been persistent and its reduction is almost unrecognized. Removal of contaminated commodities and usage of fungicides by governmental screening is one of the implementation strategies that were employed to address this issue. Reports on mycotoxin-contaminated foods still increase yearly (Stoev, 2024).

2.2. Patulin

Patulin (PAT) is a mycotoxin produced by various fungal species belonging to the genera *Aspergillus*, *Penicillium*, and *Byssochlamys* (Pillay *et al*., 2023). It is produced in various fruits and grains, notably, spoilt apples. The intergral source of PAT in mouldy apples is *Penicillium expansum* (Figure 2) (Jackson and Dombrink-Kurtzman, 2005).

Penicillium expansum is a harmful necrotrophic plant pathogenic fungus (Li *et al*., 2024). Its effects on fruits are through affecting the plant tissue through wounds, which results in the fruits decay or marceration (Wang *et al*., 2023b, Tannous *et al*., 2016). *Penicillium expansum* contamination is often recognised as blue mold (Li *et al*., 2024). Over the past years, blue mold has been detrimental to the fruit industry as it decays approximately 10% of fruit during storage (Li *et al*., 2024). *Penicillium expansum*-associated fruit decay has been linked with PAT production, which influences the poor quality of fruit production (Zhou *et al*., 2023). Long-term consumption of PAT-contaminated foods, poses an extreme risk to human health (Li *et al*., 2024, Liu *et al*., 2021a). Biocontrol of blue mold is ranked an effective method to control PAT toxicity; however, they are not ideal for use in large scale due to the environmental factors of microorganisms (Li *et al*., 2024)

PAT has been linked to various neurological, gastrointestinal, and immunological disorders resulting in damage to the liver and kidneys (Saleh and Goktepe, 2019). Previous studies have reported that PAT causes genotoxicity and teratogenicity(Mahato *et al*., 2021).

Recent studies have suggested that PAT induces cardiotoxicity; however, the pathways by which it does this have not been fully elucidated (Fan and Hu, 2024). PAT has a precursor known as 6-methyl salicylic acid that forms a part of derivatives of acetyl-CoA, both of which are polyketides and possible carcinogens (Mahato *et al*., 2021). A research study suggested that PAT caused oxidative stress that led to dysfunctional cardiac cells and cell death (Zhang *et al*., 2022a).

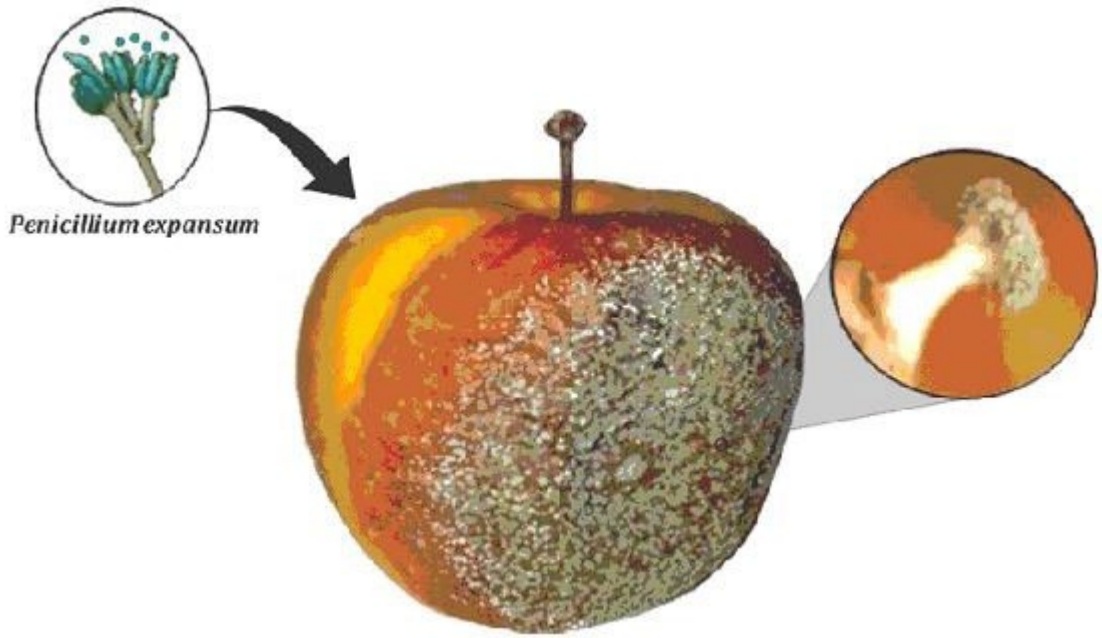

Figure 2: Patulin-contaminated apple (Li *et al*., 2024)

PAT was initially discovered as a potential antimicrobial agent in 1943 and was given the name tercinin (Saleh and Goktepe, 2019). Later, PAT was discovered as a mycotoxin because of its genotoxic, hepatoxic, and immunotoxic effects (Luciano-Rosario *et al*., 2020).

2.2.1. PAT structure and decomposition

PAT [4-hydroxy-4H-furo[3,2-c]pyran-2(6H)] is a β-unsaturated heterocyclic lactone (Figure 3) exhibiting heat-resistant properties and is stable in aqueous and acidic media (Notardonato *et al*., 2021, Luciano-Rosario *et al*., 2020). It can also survive pasteurization and is not completely destroyed during fermentation in the process of making ciders (Luciano-Rosario *et al*., 2020). Research has proven that even though PAT is soluble in many solvents including water, methanol, acetone, etc, and moderately

soluble in sulfuric acid and benzene, it can be degraded in cooking with sulfuric acid (Mahato *et al*., 2021). Furthermore, alkaline conditions destroy PAT. Another way to destroy PAT is by ultraviolet radiation; however, the damage to the fruit itself has not been determined (Mahato *et al*., 2021).

2.2.2. PAT concentration, limits, contamination control

The European Commission set the maximal patulin tolerance of 50 µg/kg, 25 µg/kg for solid apples and juice for adults, and 10 µg/kg for children's juice and other apple products (Commission, 2003). Previous studies declared the use of fungicides as a main method of controlling blue mold (Li *et al*., 2024), however, killing of fungi does not necessarily kill PAT too. Moreover, an overuse of chemical fungicides induces fungal resistance and decreases disease control since the usage of fungicides can be harmful for humans too (Eskola *et al*., 2020). Growing research has thereby provided new control methods of PAT including radiation application, the addition of food additives, and biological treatments (Tang *et al*., 2018). Modern control methods of blue mold produced by *P. expansum* includes salicylic acid application (Yu *et al*., 2020).

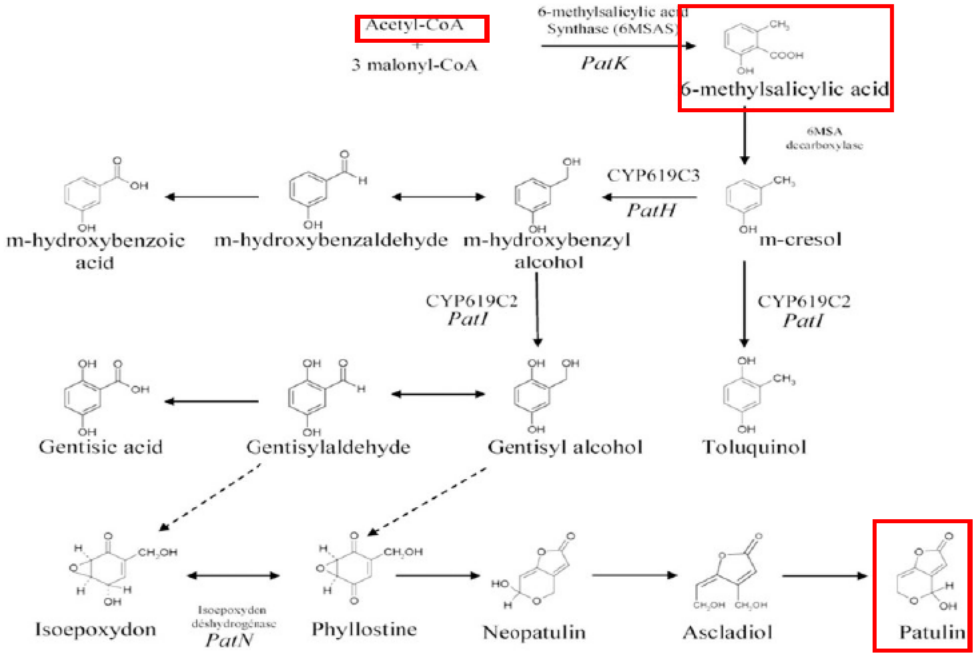

Figure 3: Biosynthesis of Patulin (Notardonato *et al*., 2021)

2.2.3. Effects of PAT

PAT has a strong affinity for sulfhydryl groups which are known to inhibit a variety of mammalian enzymes (Luciano-Rosario *et al*., 2020). When the PAT-contaminated fruit is ingested, PAT interacts with the sulfhydryl groups of glutathione and inactivates it. This results in a significant decrease in glutathione resulting in a decrease in glutathione peroxidase enzyme activity. This leads to an overproduction of ROS therefore, increasing the susceptibility of the host to oxidative stress (Notardonato *et al*., 2021, Luciano-Rosario *et al*., 2020). The induction of oxidative stress is a common pathway through which mycotoxins cause toxicities (Fan and Hu, 2024, Hsu *et al*., 2023).

2.3. Oxidative Stress

The abundant generation of reactive oxygen species (ROS) above cellular antioxidants leads to oxidative stress. It is often linked with the alteration of gene expression, which results in a variety of pathologies including diabetes mellitus, cardiovascular diseases, and neurodegenerative diseases, amongst many more (García-Guede *et al*., 2020; Hayes *et al.* 2020). This is because the accumulation of ROS causes damage to biological molecules such as proteins, DNA, RNA, and lipids, which alters biological pathways and increases the possibility of individuals being susceptible to diseases. Oxidative stress has been linked with aging, autoimmune disorders and cancer due to ROS's disruptive abilities towards DNA strand breaks, mutations, base removal, translocations and deletions (Bayr, 2005). ROS reacts with lipids and causes lipid peroxidation, yielding the lipid peroxidation end-product malondialdehyde (MDA) (Wang *et al*., 2023a). It also attacks proteins and results in amino acids oxidation, notably, sulfur-containing amino acids including methionine and cysteine thereby, altering the structure of proteins, leading to degradation and unwinding (Bayr, 2005, Juan *et al*., 2021).

2.4. Antioxidant activation

The nuclear-factor-erythroid 2-related factor 2 (Nrf2) is a master mediator and transcription factor of oxidative stress defense mechanism (Ngo and Duennwald, 2022). Its stability is regulated by Kelch-like ECH-associated protein 1 (Keap1) which is tightly bound to it for regulation of its cellular distribution (Ulasov *et al*., 2022). Studies reported that Nrf2 interacts with the antioxidant response element (ARE) and activates oxidative stress response by transcribing for relative genes such as phase II detoxification enzymes and antioxidative enzymes (Nguyen *et al*., 2003b). The induced enzymes are regulated and mediated at the transcriptional level by ARE, found in the promoter region of the enzyme's gene (Nguyen *et al*., 2009, Adinolfi *et al*., 2023). Moreover, Nrf2 is controlled transcriptionally,

translationally, and post-translationally by epigenetic modifications (Nguyen *et al*., 2003a). The Nrf2/Keap1 regulatory system is depicted in Figure 4 (Song *et al*., 2021).

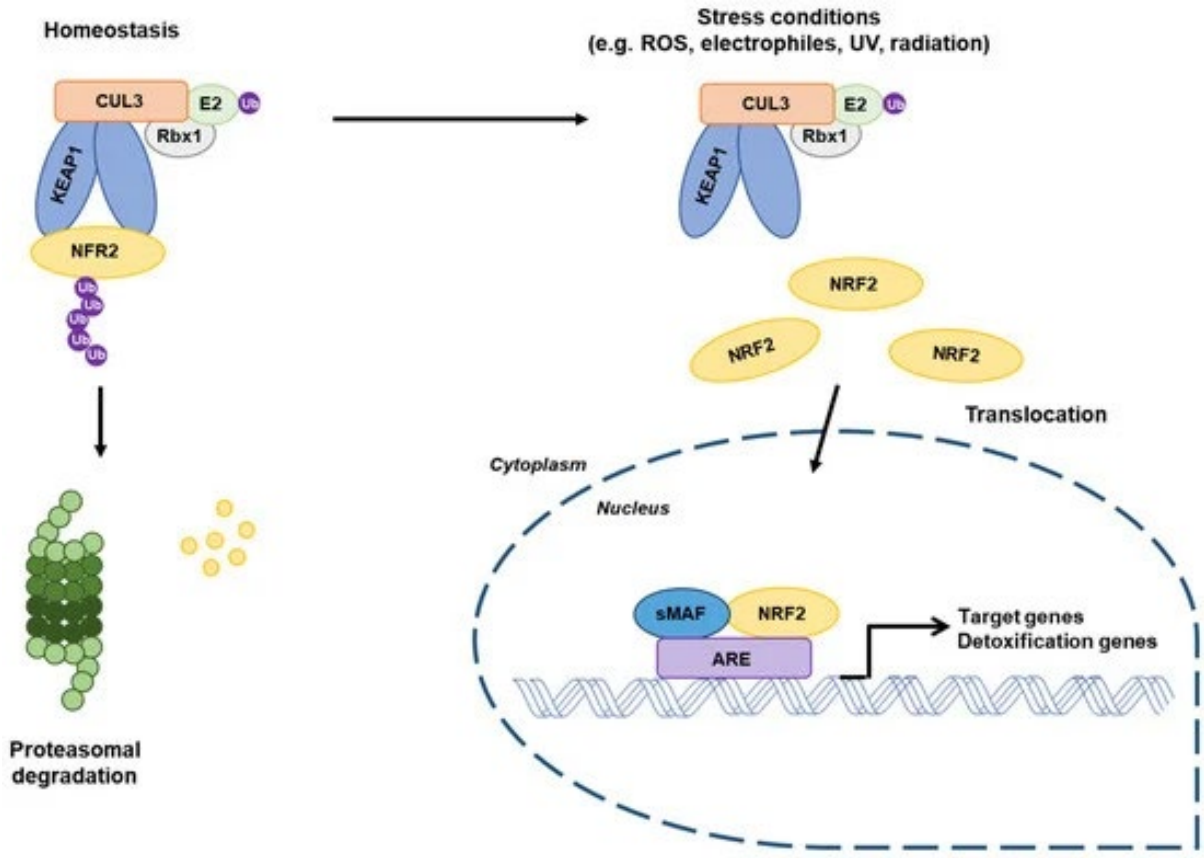

Figure 4: Regulation of Nrf2 by Keap1 (Song *et al*., 2021).

Under physiological conditions, Keap1 is bound to Nrf2 and represses its activation. Under high pH conditions, Keap1 ubiquitinates and localizes Nrf2 near the proteosome which enhances its chances for degradation inside the cytoplasm of cells (Liu *et al*., 2021b, Ngo and Duennwald, 2022). Under stressful cellular conditions where ROS levels are elevated above normal, the cysteine residues of Keap1 are oxidized, resulting in the separation of Nrf2 and Keap1, and Nrf2 translocates to the nucleus (Taguchi and Yamamoto, 2020). Inside the nucleus, Nrf2 becomes a constituent of heterodimers known as Maf proteins (Adinolfi *et al*., 2023). Thereafter, Nrf2 transcribes the antioxidant genes by interacting with the regulatory DNA that is found in the ARE (Liu *et al*., 2022). ARE regulates the activities of antioxidants and their activation in the target gene sites (Ulasov *et al*., 2022).

An activated form of Nrf2 is phosphorylated Nrf2 (*p*Nrf2). This is facilitated by Protein Kinase C (PKC) at the level of Ser40 (Huang *et al*., 2002). The domain residue for Nrf2-Keap1 interaction is Ser40 which is commonly reported as a constituent of the Neh2 (consisting of approximately 100 amino

acids). This domain of Nrf2 is bound by Keap1 while it is phosphorylated by PKC at Ser40 under oxidative stress conditions. This results in a separation of Keap1 and Nrf2 (Huang *et al*., 2002, Niture *et al*., 2014).

ROS detoxification is induced by antioxidants including, catalase (CAT), superoxide dismutase (SOD), and glutathione peroxidase (GPx) (Hayes *et al*., 2020). SOD functions as an acute response by converting superoxide ion ($O_2^{\cdot-}$) to hydrogen peroxide (H_2O_2) (Figure 5), while GPx and CAT further detoxify H_2O_2 to water (H_2O) and oxygen gas (O_2) (Figure 5) (Sies, 2020). SOD2 is alternately referred to as manganese-dependent superoxide dismutase (MnSOD). It is found on chromosome 6 in humans where it is encoded by the SOD2 gene. It functions as the superoxide radicals detoxifier that are produced by the electron transport chain in the mitochondria. Glutathione consists of an exotic amino acid namely selenocysteine inside of its active sites. Moreover, it detoxifies lipid peroxides to produce to H_2O and correlated alcohols (Pei *et al*., 2023, Birben *et al*., 2012).

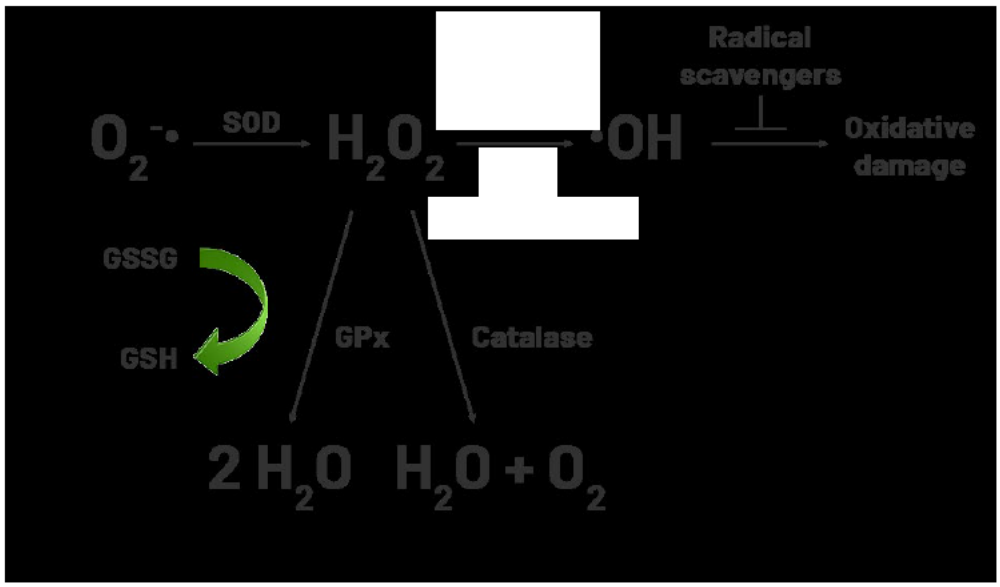

Figure 5: Oxidative stress demonstration (Korovesis *et al*., 2023).

2.5. Oxidative stress induced cardiotoxicity

Adverse effects of mycotoxin in cells include the generation of ROS and oxidative stress induction (Da Silva *et al*., 2018). This results in damage to cellular membranes, DNA, proteins, lipids and enzymes. PAT exhibits very high sulfhydryl groups' affinity, therefore, the excessive production of ROS caused by PAT toxicity may be a byproduct of the electrophilic attack towards the antioxidant enzymes consisting of the sulfhydryl group, notably, GSH (Da Silva *et al*., 2018). Health issues such as

cardiotoxicity were previously proven to be associated with the presence of oxidative stress (Zhang *et al*., 2022a).

2.6. Epigenetics

Epigenetic modification is a process in which gene expression is altered, however, the DNA sequence remains the same (Ashe *et al*., 2021). This modification contributes in the induction of diseases and cell maturation, and is achieved by various processes such as histone modifications, DNA methylation and non-coding microRNAs (Kowluru, 2023). Epigenetic modifications are reversible and can be transmitted from generation to generation (Ashe *et al*., 2021). Commonly studied epigenetic mechanisms are promoter methylation, histone modifications and DNA methylation and they are well known for their functions in regulating gene transcription through alterations of chromatin structure and DNA accessibility (Davalos and Esteller, 2023, Moore, 2013). These are influenced by external environmental factors and result in a change in phenotype (Loscalzo and Handy, 2014). The role of epigenetics in cardiovascular diseases (Handy *et al*., 2011), cancer (Chen and Yan, 2021) and neurodegenerative diseases have all been elucidated; however, the research gap remains unfilled regarding the role of epigenetics in mycotoxin-induced diseases (section 2.7, page 22).

2.6.1. Struture of chromatin

Chromatin is comprised of the nucleosome, which has about 147 DNA base pairs that are wrapped around an octamer of core histones, condensed by winding around a polynucleosome fibre (Quina *et al*., 2006). The histone core is made up of two positively charged molecules comprised of H2A, H2B, H3 and H4. Each nucleosome is linked to the next by the DNA linker. Most chromatin is further condensed by winding around the polynucleosome that is stabilized through the binding of H1 histone to each nucleosome and to the linker DNA (Quina *et al*., 2006, Kim, 2021). The chromatin structure contributes to the stability of the genome and has dynamics to counter stress factors that may influence gene expression. It has two different forms (Figure 6) - heterochromatin and euchromatin. Heterochromatin is a transcriptionally inactive form, expressed by a closed and tightly compacted chromatin. Euchromatin is a transcriptionally active form with loosely packed chromatin (Kim, 2021, Handy *et al*., 2011). The entire structure is modulated by the post-translational modifications of histone tails and the DNA (Kim, 2021).

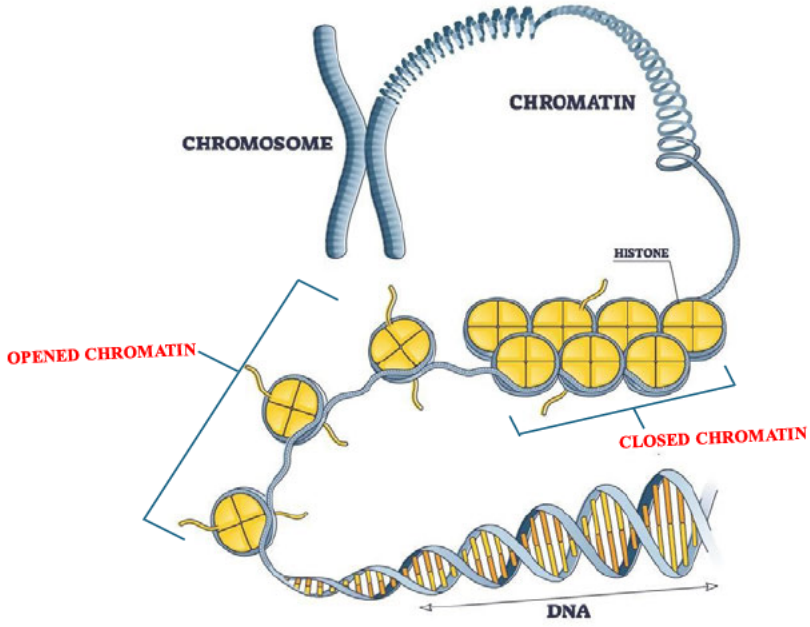

Figure 6: The structure of chromatin (Zimmer, 2021).

2.6.2. DNA methylation

DNA methylation is a biochemical process responsible for the maintenance of genome stability via gene silencing during a repressed chromatin structure (Mattei *et al*., 2022). This is an important process in cell development and differentiation. It plays a pivotal role throughout the development and differentiation of cells. It is also associated with the creation of prominent cellular lineages of the organisms (Mattei *et al*., 2022).

DNA methylation is subdivided into three different types (Li, 2021); however, the most studied DNA methylation mechanism is the gene repressing modification that occurs by transferring the methyl (CH_3) group from s-adenosyl methionine (SAM), the methyl group donor, to cytosine residues at the level of carbon five (Figure 7) (Smith *et al*., 2024, Mattei *et al*., 2022). This is catalyzed by DNA methyl transferases (DNMTs) to form 5-methylcytosine (5mC) (Figure 7) and produce thymine during the process of deamination. It also influences chromatin to tighten and obstruct the binding of transcription factors (Kowluru, 2023).

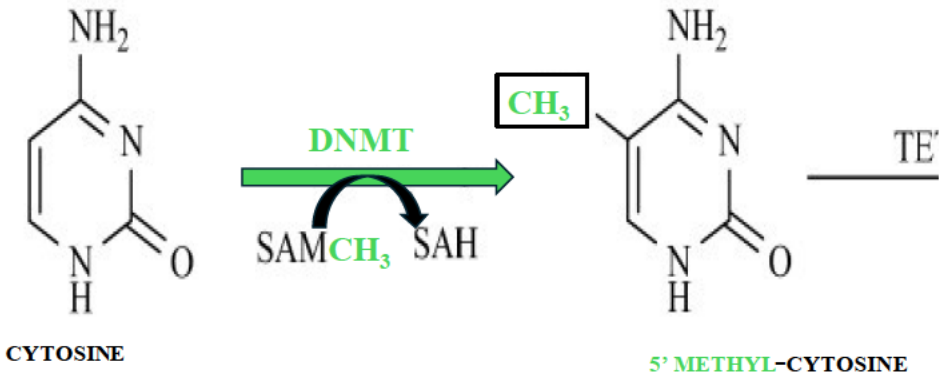

Figure 7: DNA methylation (Miranda-Duarte, 2018)

DNMT1, DNMT3A, DNMT3B and DNMT3L are the common DNMTs. The role of DNMT1 is to add a methyl group to hemimethylated strands of the DNA during replication and maintains the methylation pattern across generations (Del Castillo Falconi *et al*., 2022, Zhang *et al*., 2023). DNMT1 also has the ability to repair DNA methylation patterns (Moore, 2013), and decreased levels of DNMT1 in mice were reported to cause embryonic lethality, disruption of DNA methylation and apoptosis (Ren, 2022).

The role of DNMT3A and DNMT3B as *de novo* DNMTs is to install new DNA methylation patterns (Tajima *et al*., 2022). They are functionally active during embryogenesis and contributes to embryonic development and differentiation. Suppressed DNMT3A in mice was reported to cause death shortly after birth, while suppressed DNMT3B revealed death *in utero* with adverse developmental defects. Moreover, suppressed DNMT3A and DNMT3B revealed embryo arrest shortly after gastrulation, others faced genomic instability and vulnerability to spontaneous immortalization (Tajima *et al*., 2022, Dodge *et al*., 2005, Okano *et al*., 1999).

The role of DNMT3-like (DNMT3L) as a part of the DNMT3 family that lacks the ability to perform DNA methylation (Tajima *et al*., 2022), is to enhance the function of both DNMT3A and DNMT3B. It does this by enhancing their affinity for SAM (Kubo *et al*., 2024). DNMT3L functions to establish the paternal and maternal genomic imprinting, methylate the retrotransposons and X-chromosome inactivation (Emperle *et al*., 2021). It is commonly expressed in germ cells and throughout the developmental stages. In a male mouse study, suppression of DNMT3L resulted in distorted spermatogenesis and lack of production of mature sperm cells (Qin *et al*., 2021, Aapola *et al*., 2004, Webster *et al*., 2005). In female mice, suppression of DNMT3L resulted in embryonic lethality (Kobayashi *et al*., 2012).

2.6.3. DNMTs structural composition

The DNMT1 gene encodes for a 183 kDa protein at the level of translation and is located at chromosome 19 (19p13.2) in humans. This protein constitutes 1616 amino acids (aa), and three regions: the C-terminal region, lysine-glycine (KG)-repeats and an N-terminal region (Kikuchi *et al*., 2022). The N-terminal is a regulatory region with two bromo-adjacent homology (BAH1 and BAH2) domains, a DNMT-associated protein 1 (DMAP1) interaction domain, a cysteine-rich zinc (CXXC) binding domain, a proliferating cell nuclear antigen (PCNA) binding domain (PBD), a replication foci targeting domain (RFTD) and a nuclear localization signal (NLS) (Cheng and Blumenthal, 2008, Kikuchi *et al*., 2022). DNA methylation patterns are maintained during developmennt mainly because of the translocation of the transcriptional repressors to the replication foci by the DMAP1 domain. (Rojas *et al*., 2024).

During the process of DNA replication, DNMT1 is recruited to the replication fork by the PBD domain which has a DNA-binding motif (Rojas, 2023). The NLS functions to import DNMT1 into the nucleus (Jones *et al*., 2021) whereas the RFTD domain functions to target DNMT1 to heterochromatin and the replication foci (Kikuchi *et al*., 2022). The CXXC domain functions to bind to unmethylated CpG dinucleotides (Ren, 2022), while BAH1 and BAH2 domains are responsible for DMNT1 folding (Tajima *et al*., 2022). The C- and N-terminal regions linkage is through KG-repeats that are capable of regulating the activity and stability of DNMT1 by experiencing post-translational modifications (Kikuchi *et al*., 2022). Mediation of all interactions between DNMT1 and SAM is catalyzed by the C-terminal region. It enhances DNMT1 binding to hemimethylated CpG dinucleotides and promotes DNMT1 activity (Kikuchi *et al*., 2022). Furthermore, DNMT1 has an allosteric site, which is commonly known for its independence from the catalytic domain. Moreover, it increases its affinity for DNA and SAM by binding to 5-methylcytosine (Tajima *et al*., 2022).

The DNMT3A and DNMT3B genes which are located on chromosome 2 (2p23.3) and chromosome 20 (20q11.2), encode for 101 kDa and 130 kDa proteins during the translation process, respectively. The DNMT3A protein has 912 amino acids and DNMT3B protein has 853 amino acids. Structurally, the two proteins show similarities, however, only their length varies (Cheng and Blumenthal, 2008). Unlike DNMT1, these proteins have only N-terminal and C-terminal regions (Figure 8) (Tajima *et al*., 2022). The N-terminal consists of a DNMT3L-type zinc finger (ADD) domain and an adaptable site, proline-tryptophan-tryptophan-proline (PWWP) domain (Tajima *et al*., 2022). The PWWP domain binds to DNA non-specifically and targets DNMT3A and DNMT3B at the center of heterochromatin (Tajima *et al*., 2022, Cheng and Blumenthal, 2008). The protein-protein interactions and binding to DNMT3L are mediated by the DNMT3L-type zinc finger and

the CXXC motifs found in the ADD domain. (Tajima *et al*., 2022). The DNMT3A and DNMT3B mediated *de novo* methylation is regulated by the catalytic domain found in the C-terminal region (Tajima *et al*., 2022).

The DNMT3L gene, located on chromosome 21 (21q22.3), encodes a 44 kDa protein. The protein shows structural similarities to both DNMT3A and DNMT3B; however, it does not have the C-terminal catalytic region nor the PWWP domain (Figure 8) (Kubo *et al*., 2024).

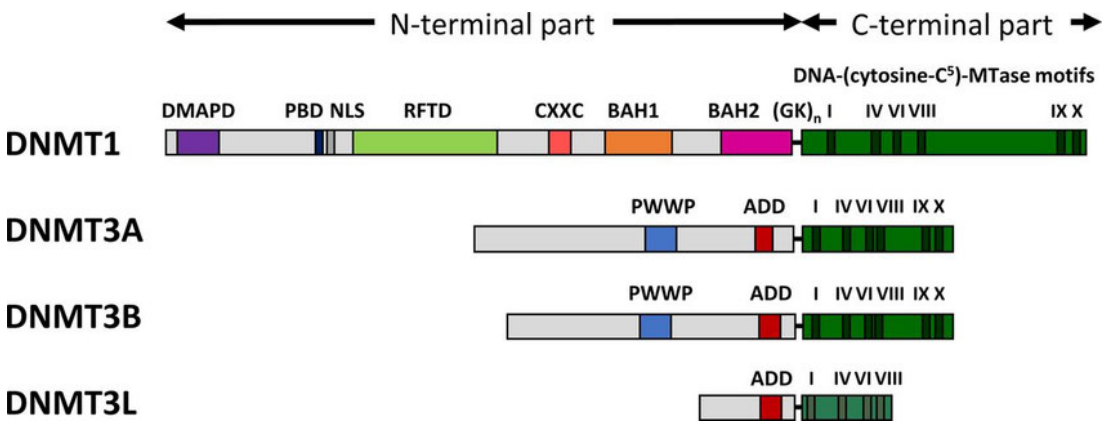

Figure 8: DNMT proteins structure (Jeltsch and Jurkowska, 2016).

2.6.4. DNMTs regulation

DNMTs are integral regulators of DNA methylation thus their expression levels influence a variety of cellular activities and patterns of DNA methylation (Del Castillo Falconi *et al*., 2022). Research has proven that dysregulation or dysfunction of DNMTs has been associated with adverse pathologies, notably, cancer (Lu *et al*., 2020, Zhu *et al*., 2024). These include breast tumours, and pancreatic and lung cancers (Zhu *et al*., 2024, Wang *et al*., 2024, Liang *et al*., 2021). These DNMT expression changes and methylation patterns were all correlated to poor health of the patients affected (Tajima *et al*., 2022).

2.6.5. Methyl-CpG binding domain proteins

Methyl-CpG binding domain (MBD) proteins are nuclear proteins responsible for DNA methylation regulation and recruit remodelling complexes of the chromatin to the methylated DNA. They also have a high affinity for 5-methylcytosine (Coelho *et al*., 2022). MBD proteins include MBD1, MBD2,

MBD3, MBD4. MBD5 and MBD6, which all play a pivotal role in the development of mammals by regulating cell division and growth, genome stability, neurogenesis and cell specialization (Du *et al*., 2015, Coelho *et al*., 2022).

MBD protein structures all comprise of an MBD that binds to methylated CpG dinucleotides and supplementary domains including the CXXC domain of MBD1, responsible for MBD1 maintaining the heterochromatin state that represses binding of both unmethylated DNA and methylated one (Figure 9) (Coelho *et al*., 2022, Du *et al*., 2015). The transcriptional repressor domain (TRD) is located in both MBD1 and MBD2 and the coiled coil (CC) domain is located in both MBD2 and MBD3; both these domains regulate protein-protein interactions and recruit proteins that repress chromatin (Figure 9) (Coelho *et al*., 2022). MBD2 has an N-terminal glycine-arginine (GR) saturated domain which is subjected to modifications post-translationally (Figure 9). Moreover, MBD2 has the most common amino acid sequence as those found in MBD3; however, MBD3 does not have the GR-saturated domain and cannot of bind to methylated DNA because of phenylalanine that substitutes tyrosine at the level of MBD domain (Figure 9) (Magdinier and Wolffe, 2001, Coelho *et al*., 2022). MBD4 functions to repair mismatched DNA and has a C-terminal glycosylase domain (Figure 9) that enables it to perform its function (Coelho *et al*., 2022). Both MBD6 and MBD5 comprise of a proline-saturated domain and a PWWP domain that bind to histones that are methylated and regulate closed chromatin (Figure 9) (Coelho *et al*., 2022, Du *et al*., 2015).

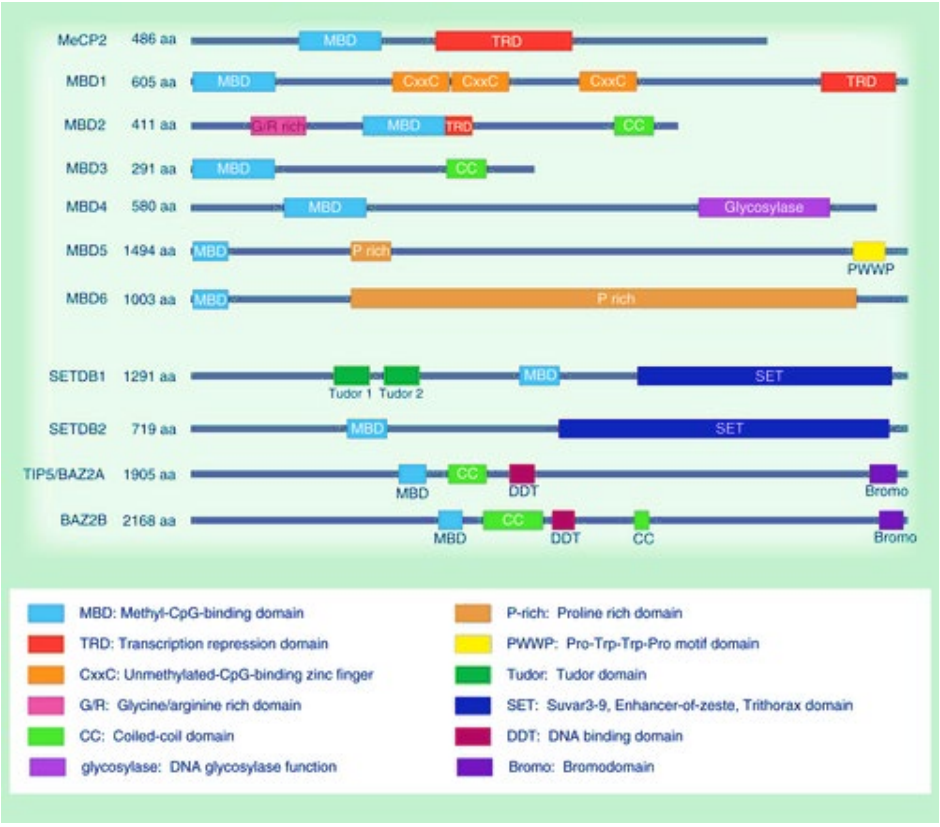

Figure 9: MBDs structure (Du *et al*., 2015).

2.6.6. MBD2

The significant protein of the MBD family is MBD2. It attaches to methylated DNA to function as a DNA demethylase and a methylation-dependent transcriptional repressor (Wood and Zhou, 2016). This is the only MBD in the MBD family that can do this. It is associated with pro-metastatic gene activation (Schmolka *et al*., 2023) and its suppression results in inhibition of proliferation of cells while its overexpression results in tumorigenesis through DNA hypomethylation, disruption of the genome and silenced tumour suppressor genes (Magdinier and Wolffe, 2001, Wood and Zhou, 2016, Zhang *et al*., 2023). Mouse studies have revealed that suppression of MBD2 results in defective neurogenesis and disruptive maternal behaviour (Hendrich *et al*., 2001).

2.7. Mycotoxicology and epigenetics

Mycotoxin-contaminated food consumption has been rapidly reported to be associated with adverse health issues. After consumption, the breakdown of these mycotoxins leads to its conversion to toxic metabolites which react with different biomolecules, resulting in defects (Awuchi *et al*., 2022). Recent studies provided insights of mycotoxin effects on epigenetics (Chen and Yan, 2021, Li *et al*., 2023, Sugiyama *et al*., 2021, Zhu *et al*., 2021)

PAT has been reported to be associated with causing nephrotoxicity by altering global DNA methylation and alpha-adrenergic receptor signalling in C57BL/6 mice (Mazibuko *et al*., 2024). Recently, in 2021, South Africa and its neighbouring countries, namely Zimbabwe, Zambia, Democratic Republic of Congo, Uganda, and Kenya, experienced a significant incident of PAT contamination in products sold by Pioneer Foods. This led to the recall of several apple juice products, including Appetiser, due to PAT levels exceeding the regulatory limit of 50 µg/L. The recall of these products negatively impacted the economy and increased the risk for adverse health effects in individuals that had already consumed these products.

Fumonisin B_1 is a chemical compound produced by the fungal species *Fusarium* and has been associated with global DNA hypermethylation through an increase in DNMTs activity (Sugiyama *et al*., 2021).

Aflatoxins are a group of mycotoxins that have a subgroup namely aflatoxin B_1, which is produced mainly by *Aspergillus flavus* and *Aspergillus parasiticus* (Dai *et al*., 2017). Previous studies have shown

that aflatoxin B_1 has been involved in causing epigenetic alteration, notably, DNA methylation by increasing DNMTs (Dai *et al*., 2017, Rotimi *et al*., 2021, Liu *et al*., 2023a).

Ochratoxin A is a food-contaminating fungal toxin well known as a rat renal carcinogen (Ozawa *et al*., 2024). It has also been previously proven to induce DNA methylation by altering the promoter-region methylation process in proximal tubular epithelial cells (Ozawa *et al*., 2023).

Zearalenone is a mycotoxin produced by the species Fusarium and was reported to also show changes in DNA methylation by inducing genome toxicity (Feng *et al*., 2022).

Therefore, knowing the in-depth mechanisms, through oxidative stress and DNA methylation changes, by which PAT affects human health is significant to help resolve the undying issue of mycotoxin contamination.

CHAPTER 3: METHODOLOGY

3.1. Materials

PAT (P1639) was bought from Sigma-Aldrich (Missouri, USA). Primer sequences were bought from Inqaba Biotechnical Industries (Pty) Ltd (Pretoria, South Africa). Methylated DNA quantification kit (catalogue no. ab117128) was purchased from Abcam (Cambridge, UK). All western blotting reagents and equipment were obtained from BioRad (Hercules, California, USA) and Cell Signalling Technology (Danvers, Massachusetts, USA). All other reagents were acquired from Merck (Darmstadt, Germany) unless stated otherwise.

3.2. Animal Treatment

Ethics was obtained from the University of KwaZulu-Natal Animal Research Ethics Committee (ethics number: AREC/079/016; Appendix A). In accordance with ARRIVE guidelines, all experiments were conducted. Male C57BL/6 mice were housed at the Africa Health Research Institute under laboratory conditions of 40-60% humidity, 25°C, and a 12 hrs light-dark cycle. All mice were fed food and water for the duration of the study. The mice, each weighing 20-22g, were separated spontaneously into two groups (n=5 per group): (1) control group (administered with 0.1M PBS, 24 hrs) and (2) PAT treated mice (administered with 2.5 mg/kg PAT, 24 hrs). All treatments were orally administered by gavage.

The treatments for control and experimental animals were not repeated; this was in keeping with the ethical approval from the University of KwaZulu-Natal. After a once off treatment, the mice from both groups were sacrificed by cardiac puncture. The hearts were rinsed in 0.1M PBS after their harvest and stored in 500 µl Cytobuster reagent (Novagen, San Diego, CA) for protein isolation and 500 µl Qiazol reagent (Qiagen, Hilden, Germany) for RNA isolation. An overview of the mice treatments is depicted in Figure 10. All samples were stored in (-80ºC) until ready to be assayed. An overview of the experimental design is depicted in Figure 10.

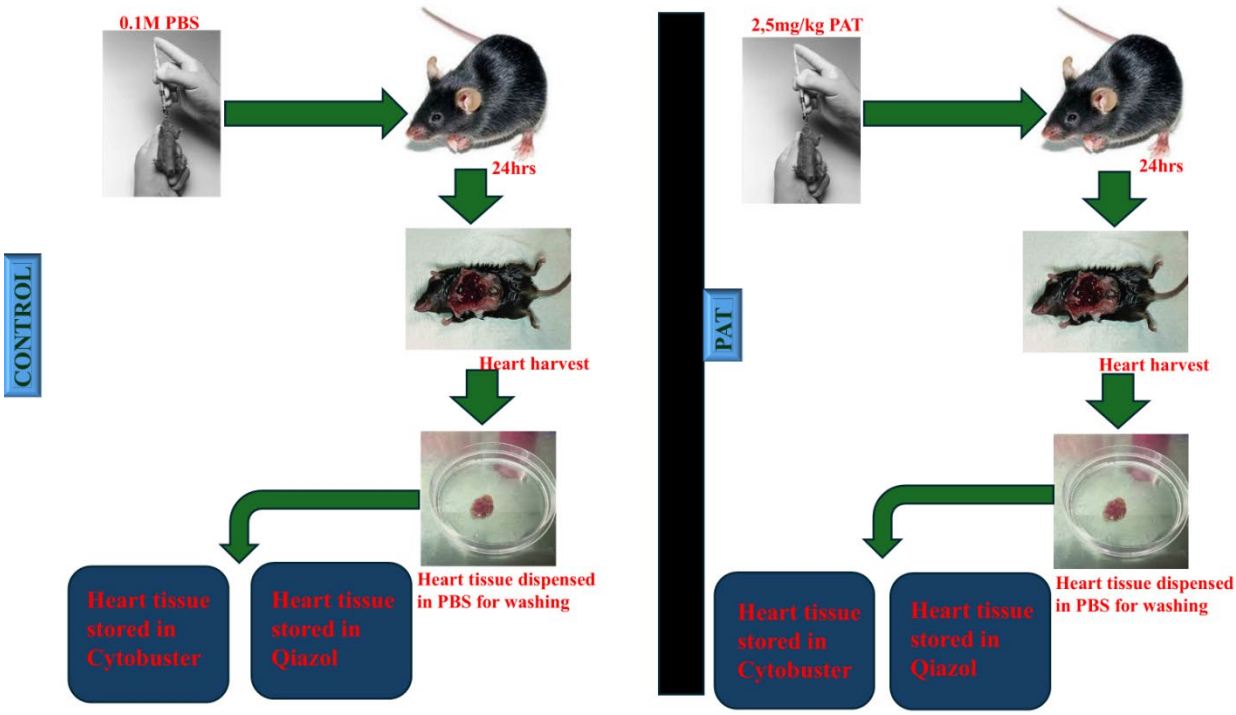

Figure 10: Mice treatment and mice sacrifice (Prepared by author)

3.3. Tissue Preparation

The harvested mice were thawed, and each heart was homogenized using a Dounce homogenizer. The homogenates were centrifuged (10000 xg, 4ºC, 10 min) and the supernatants were retained for RNA and protein isolation and stored at -80ºC, which were later used for qPCR and western blot.

3.4. Gene expression

Introduction

Quantitative polymerase chain reaction (qPCR) rapidly amplifies and quantifies a specific gene from a template strand (Hunter *et al*., 2010). The thermocycler machine is used in this protocol for incubation at three different steps and corresponding different temperatures and is measured in cycles. The three steps involved are denaturation, annealing and extension (Figure 11). During denaturation, a natural form of DNA unfolds, and separate resulting is singular DNA strands at. During annealing, the template DNA is recombined with primers complementary to the target sequence. During extension, DNA polymerase (Taq DNA Polymerase) extends the annealed primers. A complete cycle is composed of all

three stages and each cycle amplifies the target copy. Each cycle is repeated 30-40 times for sufficient amplification (Pestana *et al*., 2010) resulting in over 10X fold of amplification from the template DNA.

For PCR to take place, the following needs to be present:

- A DNA template constituting the sequence of interest.
- A buffer system which will maintain the optimized pH of PCR
- The sense and antisense primers which will adhere on the 3' terminals of both the sense and antisense strands of the sequence of interest.
- $MgCl_2$ which will stabilize the DNA and ensure optimized Taq polymerase functioning by acting as a cofactor of Taq polymerase.
- A Taq polymerase which will add nucleotides onto the terminals of the primers that underwent annealing process, catalysing the composition of a new complementary DNA strands to the sequence of interest.
- Deoxynucleotide triphosphatases (dNTPs) which will facilitate the composition of new strands (these are the building blocks).

The qPCR method can quantify the amplicons of PCR and measure them as they are generated during each cycle (Pestana *et al*., 2010). The amplicons are detected with SYBR® Green, a DNA-intercalating dye. The intensity of the dye gets stronger when attached to the shallow grooves found in the double stranded DNA. Therefore, the intensity of fluorescence and the present double stranded DNA are directly proportional (Pestana *et al*., 2010).

Samples are analysed for the expression of the gene of interest and the housekeeping gene. In each sample, the total target DNA is expressed in correspondence with the total housekeeping gene. The analysis of gene expressions is then performed employing the Livak and Schmittgen ($2^{-\Delta\Delta CT}$) method and presented as fold change relative to the control.

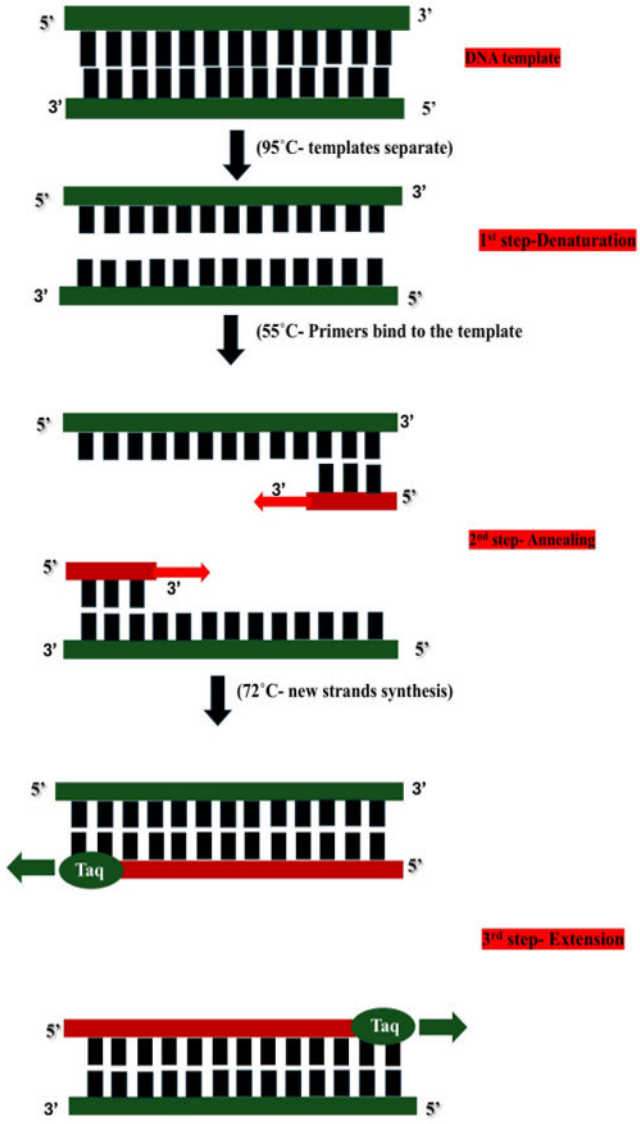

Figure 11: DNA amplification - PCR cycle (Prepared by author).

3.4.1. RNA Isolation

Protocol

The supernatant from samples that were previously stored in Qiazol and homogenized were thawed at room temperature and chloroform (100 µl) was added. The samples were shaken vigorously for approximately 15 seconds, then incubated for 2-3 minutes at room temperature followed by centrifugation for 15 minutes at 12000 xg, 4°C. The aqueous solutions that have crude RNA were

transferred into fresh 1.5 ml microcentrifuge tubes. Each 1.5 microcentrifuge tube was added with isopropanol (250 µl) and flicked well to mix. An incubation (1 hr, -80°C) of samples was followed by centrifugation (20 min, 12000x g, 4°C). The supernatants were removed, and the pellets were washed with 500 µl of 75% cold ethanol. The samples were centrifuged (15 min, 7400 xg, 4°C) and ethanol was thoroughly removed so that the pellets dry off (approximately for 30 minutes). Each RNA pellet was resuspended to nuclease-free water (15 µl) incubated for 2-3 minutes, and stored at -80°C (Ghazi et al., 2022).

3.4.2. cDNA synthesis

Protocol

RNA samples were quantified using a Nanodrop2000 spectrophotometer (Thermo-Fisher Scientific, Waltham, US) and standardized to 1000 ng/µl. cDNA was synthesised using the Maxima H Minus cDNA Synthesis Kit (Thermo-Fisher Scientific, Waltham, US) (Ghazi et al., 2022). A master mix was prepared by adding nuclease-free water (12.75 µl) to 10 mM dNTP mix (1 µl) and Oligo $(dT)_{18}$ primer (25 mol, 0.25µl). In five fresh 200 µl micro-centrifuge tubes, 14 µl of the master mix was added with 1 µl of template RNA. This was mixed and incubated for 5 minutes at 65°C using a thermo-cycler. Samples were then chilled on ice before adding 5X RT buffer (4 µl) and maxima H minus enzyme mix (1 µl). The samples were incubated for 10 min at 25°C, followed by 15 min at 50°C. This reaction was terminated by heating at 85°C for 5 min using a thermo-cycler. Nuclease-free water (60 µl) was added to the samples, and stored at -80°C.

3.4.3. Qualitative Polymerase Chain Reaction (qPCR)

Protocol

Using the PowerUp™ SYBR™ Green Master Mix (Thermo-Fisher Scientific, Waltham, US), the gene expression analysis was conducted (Ghazi et al., 2022). The mRNA expressions of Keap1, NRF2, GPx, SOD2, CAT, MBD2, DNMT1, DNMT3A and DNMT3B were determined using the sense (forward) and antisense (reverse) primers listed in Table 2. A housekeeping gene, GAPDH was utilized to normalize the genes. SYBR green (5 µl), sense primer (1 µl), antisense primer (1 µl), nuclease-free

water (2 µl) and cDNA template (1000 ng/µl, 1 µl) were constituents of reactions with different volumes and these were carried out in triplicates.

QuantStudio 3 Real-Time PCR System (Thermo-Fisher Scientific, Waltham, US) was employed to amplify the samples. The $2^{-\Delta\Delta CT}$ method determined the changes in gene expression.

Table 2: Primer sequences and annealing temperatures

Gene	**Sense (S) or Antisense (AS)**	**Sequence**	**Annealing temperature (°C)**
Keap1	S	5'-ATCCAGAGAGGAATGAGTGGCG-3'	58
	AS	5'-TCAACTGGTCCTGCCCATCGTA-3'	
NRF2	S	5'-CTTTAGTCAGCGACAGAAGGAC-3'	58
	AS	5'-AGGCATCTTTGTTTGGGAATGTG-3'	
GPx	S	5'-AGTCCACCGTGTATGCCTTCT-3'	59
	AS	5'-GAGACGCGACATTCTCAATGA-3'	
SOD2	S	5'-AGACCTGCCTTACGACTATGG-3'	59
	AS	5'-CTCGGTGGCGTTGAGATTGTT-3'	
CAT	S	5'-TGGCACACTTTGACAGAGAGC-3'	60
	AS	5'-CCTTTGCCTTGGAGTATCTGG-3'	
DNMT1	S	5'-AGAGACCAGGATAGGAAACGCA-3'	60
	AS	5'-CTCCTTTGATTTCCGCCTCAAT-3'	
DNMT3A	S	5'-GGCCGAATTGTGTCTTGGTG-3'	60
	AS	5'-CCATCTCCGAATCACATGAC-3'	

DNMT3B	S	5'-AGCGGGTATGAGGAGTGCAT-3'	60
	AS	5'-GGGAGCATCCTTCGTGTCTG-3'	
MBD2	S	5'-AGAACAAGGGTAAACCAGACCT-3'	58
	AS	5'-ACTTCACCTTATTGCTCGGGT-3'	
GAPDH	S	5'-AGGTCGGTGTGAACGGATTTG-3'	_
	AS	5'-TGTAGACCATGTAGTTGAGGTCA-3'	

3.5. Enzyme-linked immunosorbent (ELISA) assay

Principle

The ELISA assay principle states that specific antibodies attach to the target antigen and detect the presence and quantity of the antigen (Figure 12). The colourless substrate is converted into a colourful product, suggesting that antigen-antibody binding is present. This is facilitated by an enzyme reaction.

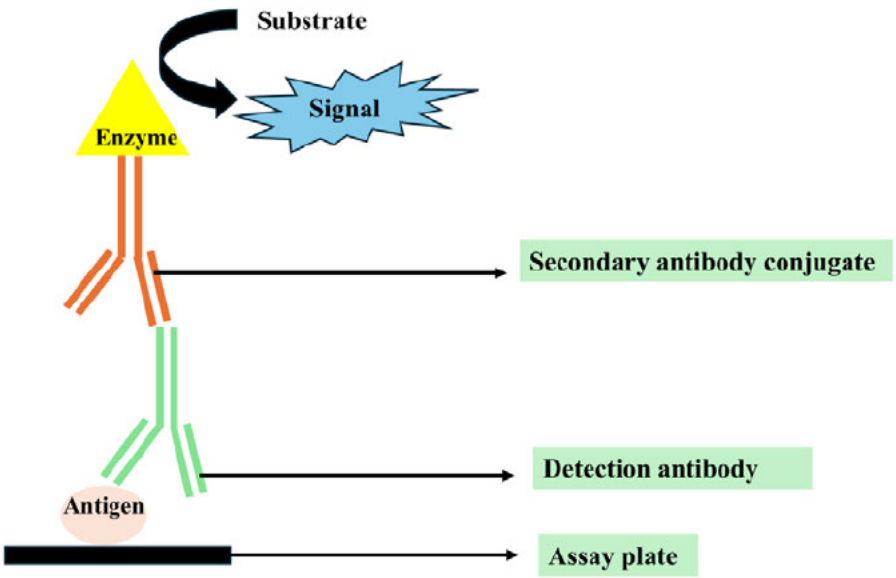

Figure 12: ELISA principle (Prepared by author)

Protocol

3.5.1. Reagent preparation

All reagents were freshly prepared on the day of use. A 1X wash buffer was prepared using 117 ml distilled water and 13 ml of 10X wash buffer making a 200 ml solution. The pH was adjusted to 7.2 – 7.5. Standard curve preparation was obtained by diluting the positive control (from the kit) to 0.5, 1, 2, 5 and 10 ng/µl according to Table 3.

Table 3: Dilution chart of positive control with 1X TE buffer

Tube	Positive control (µl)	1x TE (µl)	Final concentration (ng/µl)
1	1.0	19.0	0.5
2	1.0	9.0	1.0
3	1.0	4.0	2.0
4	2.5	2.5	5.0
5	4.0	0.0	10.0

3.5.2. Sample preparation

3.5.2.1. DNA isolation

DNA precipitate was acquired by isolating the DNA through separation of interphase and phenol-chloroform phase leftover after RNA isolation (Feezor *et al*., 2004). Excess aqueous phase overlying the interphase was removed to enhance the DNA quality. 100% ethanol (300 µl) was added and the solution was mixed by inverting the tubes several times. The solution was incubated at room temperature for 2-3 minutes and centrifuged for 5 minutes at 4˚C at 2000 xg to pellet the DNA. DNA pellet was washed in 50 µl of 0.1 M sodium citrate in 10% ethanol (pH 8.5), incubated for 30 minutes and mixed by gentle inversion. It was then centrifuged for 5 minutes at 4˚C at 2000 xg. Thereafter the supernatant was removed using micropipettes and the DNA pellet was resuspended in 1000 µl of 75% ethanol. DNA was then incubated for 10-20 minutes, mixing occasionally by gentle inversion, and then centrifuged for 5 minutes at 4˚C at 2000xg. Supernatant was removed using the micropipettes and pellets were air-dried.

The pellet was resuspended in 100 µl of 8 mM NaOH by pipetting up and down and centrifuged for 10 minutes at 4˚C at 12000 xg for removal of insoluble materials. The supernatant was transferred to a new tube and 1 mM EDTA was added.

DNA concentration was determined using the Nanodrop 2000 spectrophotometer and the 260/280 nm absorbance was used to determine sample purity. A ratio of 1:8 was considered pure.

3.5.3. ELISA procedure

The quantification of global DNA methylation was carried out using an ELISA kit (ab117128, abcam, Cambridge, UK) (Ghazi et al., 2019). Binding solution (80 µl) was added to every strip well in a 96-well plate that was to be used. Thereafter, 1 µl of negative control (from the kit) and 1 µl of the positive control standards (prepared as per Table 3), and 4 µl of sample DNA were plated. It was covered and incubated for 90 minutes at 37°C. Afterwards, the binding solution was discarded from all wells and 3 washes were performed with 150 µl of 1X wash buffer.

A 50 µl diluted capture antibody (1:1000 with 1X wash buffer) was added to each well and the plate was sealed for incubation at room temperature for 60 minutes. The diluted capture antibody was then removed and 50 µl of the diluted detection antibody (1:2000 with 1X wash buffer) was added and incubated for 30 minutes at room temperature. The detection antibody was then removed, and each well was washed 4 times with 150 µl of 1X wash buffer. A 50 µl diluted enhancer solution (1:5000 with 1X wash buffer) was added to each well and the plate was covered for 30 minutes of incubation at room temperature. It was then removed from each well and all wells were washed 5 times with 150µl of 1X wash buffer.

Each well was filled with 100 µl of developer solution and the plate was incubated for 1 to 10 minutes away from the light, monitoring the colour change in all wells. The developer solution turned blue (which usually happens in the presence of methylated DNA) and 100 µl of stop solution was added to stop the enzyme reaction. The colour then changed to yellow, and absorbance was read at 450 nm within 2-15 minutes using the microplate reader.

To quantify the amount of DNA that was methylated, the standard curve was plotted using the OD values = of the positive control standards. The slope of the standard curve was determined using the linear regression. Then the percentage of the methylated DNA (5-mC) in total DNA, using the formulae below, was calculated:

- 5-mC (ng)= $\frac{(sample\ OD - Negative\ control\ OD)}{Slope\ X\ 2}$
- 5-mC % = $\frac{5-mC\ amount\ (ng)}{S}\ X\ 100\%$

Key: S= amount of sample DNA in ng

2 is a factor to normalize 5-mC in the positive control to 100% (as the positive control contains only 50% of 5-mC) (Reen, 1994)

3.6. Thiobarbituric Acid Reactive Substances (TBARS) Assay

Introduction

The TBARS assay is a simple assay used to quantify lipid peroxidation (De Leon and Borges, 2020). The use of this assay originated from Kohn and Liversedge's work in 1944 where they measured oxidation in lipid systems. (Ghani *et al*., 2017, Kohn and Liversedge, 1944). This procedure requires acidic (pH=4) and hyperthermal conditions (95˚C) to enable the unstable pure malonaldehyde (MDA) to be released from the MDA bis (dimethyl acetal) (De Leon and Borges, 2020).

Principle

This assay measures the reaction between TBA and the byproduct of lipid peroxidation, malondialdehyde (MDA) (Figure 13). This results in a red-pink-coloured complex that can be measured spectrophotometrically at a wavelength of 532 nm. The colour intensity is acquired relative to the amount of lipid peroxidation.

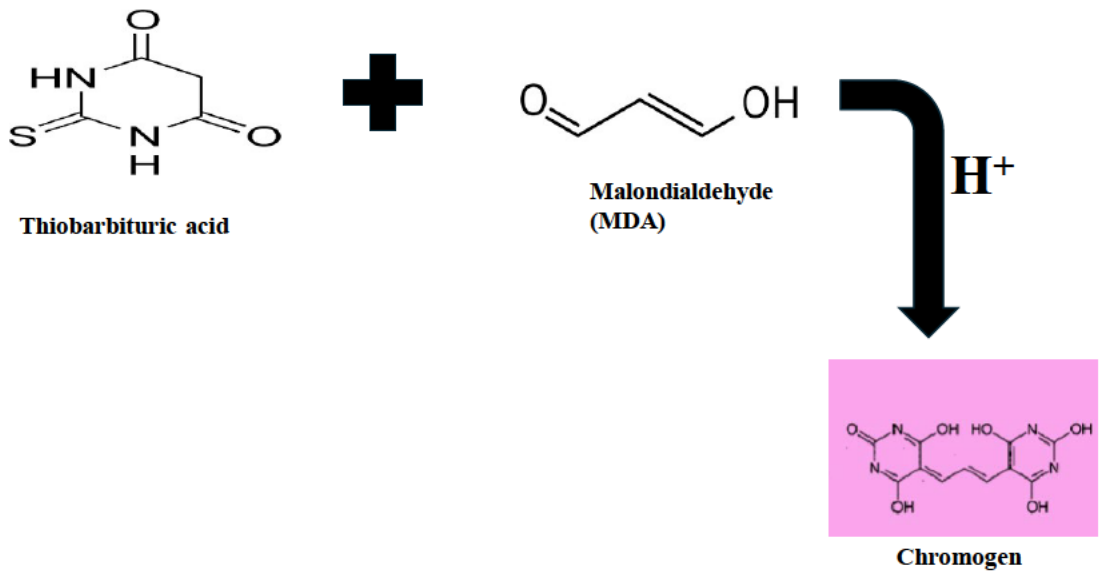

Figure 13: Principle of TBARS (Prepared by author).

Protocol

The C57BL/6 mice hearts were homogenized in PBS and supernatants were retained for TBARS assay. Ten test tubes, each with 200 µl of supernatant were prepared. In addition to that, a 1 µl MDA (positive control) and 400 µl 3 mM HCl (negative control) was prepared. Prepared 200 µl of 7% phosphoric acid was added to all tubes as well as 400 µl TBA/BHT and solutions were vortexed. The addition of TBA/BHT was not included to the negative control. The pH was lowered to 1.5 by adding 200 µl 1 M HCl and all samples were boiled in a water bath at 100°C for 15 minutes. Tubes were left to cool before adding 1500 µl of butanol and vortexed for 30 seconds to enable the separation of two heterogeneous phases. Thereafter, 100 µl of the butanol supernatants were plated into a 96-well microtiter plate in triplicates for each sample and absorbance was measured at 532 nm with a reference wavelength of 600 nm (Suthiram et al., 2023). MDA levels were calculated using the equation: MDA levels (µM) = (Absorbance/156mM) x 1000 to measure lipid peroxidation/oxidative stress in the cell.

3.6. Western Blotting

Western blot is a qualitative method that uses the antigen-antibody binding principle for the detection and quantification of specific proteins in samples (Eslami and Lujan, 2010). This technique firstly separates proteins according to their molecular weight in the sodium dodecyl sulphate polyacrylamide gel electrophoresis (SDS-PAGE). During this process, an applied voltage causes the proteins to drift toward the electrode through a gel matrix. This is because the proteins have a negative charge in them and the electrode has a positive charge (Smith *et al*., 2022). Following completion of the electrophoresis process, electro-transferring of proteins is conducted to transfer them onto a nitrocellulose membrane which will be blocked in a buffer deterring attachment of non-specific proteins. Thereafter, immunoblotting of the membrane is conducted with the desired primary antibody and their corresponding enzyme-conjugated secondary antibody to form bands representing the protein expression. This makes the target proteins easily detectable and quantifiable in a sample with a variety proteins (Sule *et al*., 2023). Western blot assessed the expression of the MBD2, DNMT3A, DNMT1, NRF2, GPx, CAT, and SOD2 proteins.

Protein isolation, standardization, gel preparation, SDS-PAGE, transfer, blocking and immunoblotting was performed as previously published (Ghazi et al., 2019).

3.6.1. Isolation of proteins

Introduction

Crude protein was isolated directly from the C57BL/6 mice hearts using the non-ionic Cytobuster™ Protein Extraction Reagent (catalogue no. 71009, Novagen, San Diego, CA). Cytobuster consists of detergents that lyse the cell membranes and result in emission of proteases and phosphatases that destroy proteins of the cell. Degradation of proteins by these enzymes is avoided by supplementation of the Cytobuster reagent with protease and phosphatase inhibitors that inactivate proteolytic and phospholytic enzymes. This increases the protein integrity and prevent their denaturation.

Protocol

The C57BL/6 mice control and PAT-treated hearts were homogenized in 500 µl Cytobuster (Novagen, catalogue no. 71009) supplemented with phosphatase (Roche, catalogue no. 04906837001) and protease inhibitors (Roche, catalogue no. 05892791001) and centrifuged (10 000 xg, 4ºC, 10 min). The supernatants with crude protein extracts were transferred into 1.5 ml microcentrifuge tubes. Pellets were discarded.

3.6.2. Standardisationof proteins and quantification

Introduction

The bicinchoninic acid (BCA) assay was employed to quantify total crude protein and was initially invented in 1985 by Paul K. Smith.

Principle

This is a colorimetric assay based on the biuret reaction in which cupric (Cu^{2+}) ions are converted to cuprous (Cu^{+}) ions in an alkaline medium (He, 2011). The Cu^{2+} ion reacts with the peptide bonds in the

proteins and is reduced to Cu^{+} ion. The newly formed Cu^{+} ion then reacts with two molecules of BCA to form a BCA-Cu^{+} complex exhibiting a purple colour (Figure 14). (Kader and Liu, 1997).

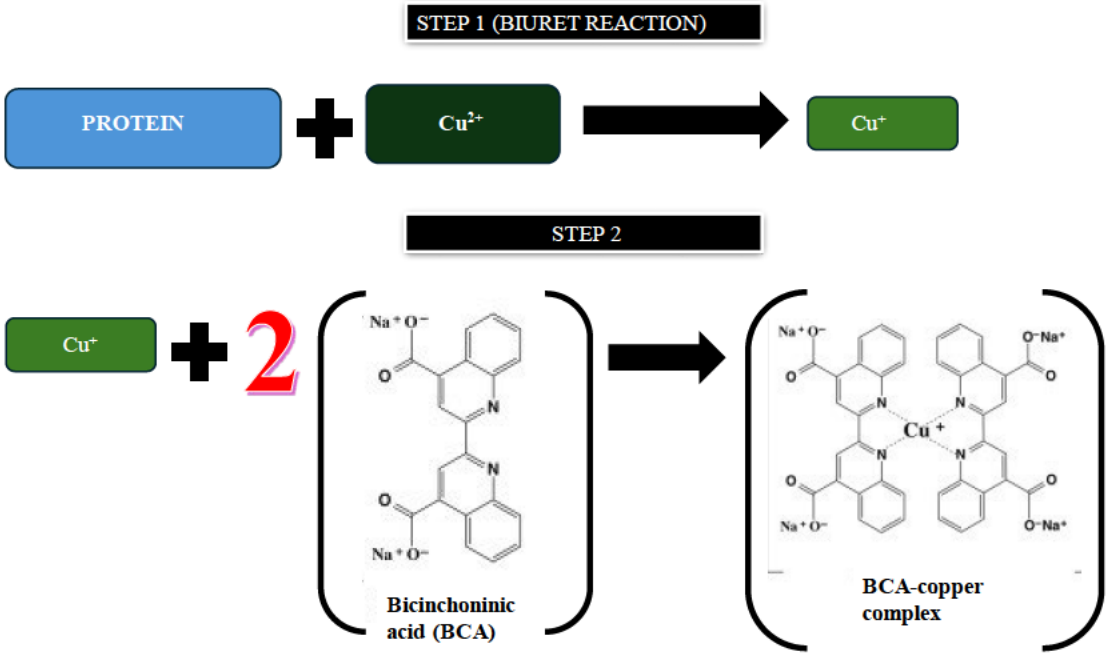

Figure 14: BCA assay principle (prepared by author).

Protocol

A range of bovine serum albumin (BSA) standards (0, 0.2, 0.4, 0.6, 0.8, and 1 mg/ml) were made with deionized water. Thereafter, each standard was plated in triplicate (25 µl) and protein samples were plated in duplicates in a 96-well microtiter plate. BCA (200 µl) working solution (4 µl $CuSO_4$ and 198 µl BCA) was pipetted into each well and the plate was incubated at 37ºC, for 30 minutes. The spectrophotometer (Bio-Tek µQuant Plate Reader) presented the absorbance results at 562 nm. A standard curve was constructed using the absorbances of the BSA standards, from which concentrations of each protein sample were calculated (Appendix B).

Proteins were later standardized to 1 mg/ml in Cytobuster reagent and boiled (100ºC) for 5 min in laemmli buffer [dH_2O, 0.5M Tris-HCl (pH 6.8), 3% glycerol, 10% SDS, 5% β-mercaptoethanol, 1% bromophenol blue]. The constituents of the laemmli buffer functions as follow: Tris-HCL maintains the pH, glycerol increases the weight of the samples to facilitate them sinking into the wells of SDS-PAGE gel (Mitacek *et al*., 2023), and bromophenol blue promotes visualization of the samples as they migrate through the gel in SDS-PAGE. SDS reduces and unfolds proteins to separate them solely based on their size (Mahmood and Yang, 2012). β-mercaptoethanol breaks down the disulphide bonds and further

reduces the proteins and exacerbates their denaturation. Samples were then cooled to RT before storing at -20^{o}C until loaded in the SDS-PAGE gel.

3.6.3. Gels preparations for SDS-PAGE

Introduction

The polyacrylamide gels are a 3D polymer prepared using acrylamide and cross-linker namely N, N' -methylene bis-acrylamide catalysed by ammonium persulfate (APS). SDS-PAGE uses two types of agarose gels to separate proteins based on their molecular weights. The bottom gel, known as the resolving gel, has a pH of 8.8 with intense polyacrylamide content that enables the SDS-PAGE gel to have narrow holes that facilitate protein separation based on their sizes (Hnasko and Hnasko, 2015). The top gel, known as the stacking gel, has a pH of 6.8 and less polyacrylamide concentration that enables the SDS-PAGE gel to have large holes in which proteins are poorly separated. Instead, the stacking gel enables the formation of sharply defined protein bands which are further separated by the resolving gel as they migrate (Kim, 2017).

Protocol

The Mini-PROTEAN Tetra Cell casting stand (Figure 15) was used to prepare the gels. A 10% resolving gel was made [dH_2O, 1.5M Tris-HCl (pH 8.8), 10% (w/v) SDS, 30% acrylamide/bis, 10% APS (freshly prepared daily), TEMED] and added between the glass plates. Isopropanol was added on top of the resolving gel to ensure a smooth surface, and it was allowed to set for 60 minutes. Once the gel was set and the gel-isopropanol phases were distinct, isopropanol was removed using filter paper. A 4% stacking gel [dH_2O, 0.5M Tris-HCl (pH 6.8), 10% (w/v) SDS, 30% acrylamide/bis, 10% APS, TEMED] was added on top of the resolving gel in between the glass plates and a 1 cm plastic comb (Bio-Rad) (Figure 15) was immediately placed in the stacking gel to form sample loading wells (Figure 16). It was allowed to set for 40 minutes.

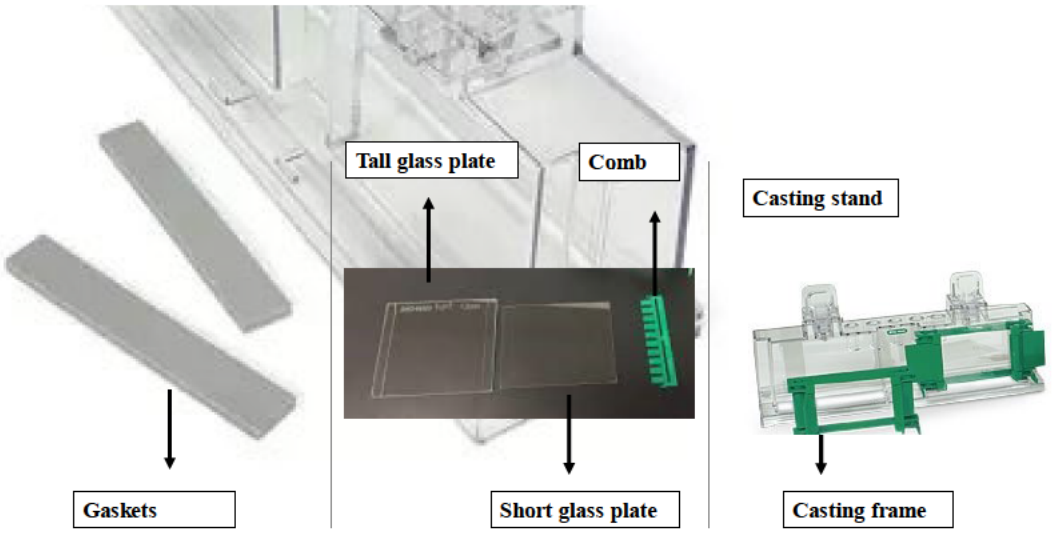

Figure 15: SDS-PAGE gel apparatus (Prepared by author).

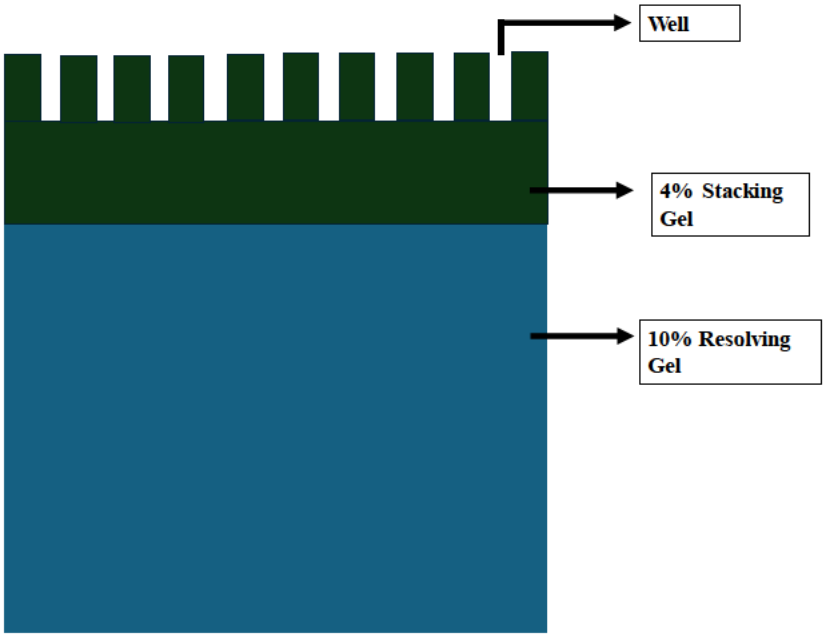

Figure 16: Typical SDS-PAGE gel (Prepared by author).

3.6.4. SDS-PAGE

After the gels had set, they were taken out of the casting stands and transferred to the electrode assembly inside the electrode tank. The electrode tank (Mini-PRPTEAN Tetra Cell System, Bio-Rad, Hercules. CA) was filled with running buffer (192 mM glycine, 25 mM Tris, 0.1% SDS). Using a loading guide, 5 µl of molecular weight marker (catalogue no. #161-0373, Bio-Rad, Hercules, CA) and 25 µl of protein samples were loaded into sodium dodecyl sulphate-polyacrylamide gels, and the apparatus was sealed. The tank was connected to a Bio-Rad compact power supplier to apply 150V for 60 minutes. Proteins were separated and the run was monitored to ensure that the tracker dye does not exceed the bottom of the gel.

3.6.5. Transfer of proteins

Gels were then transferred into transfer buffer (20% methanol, 25 mM Tris, 192 mM glycine; pH 8.3) after being carefully removed from glass plates allowing gel and protein equilibration. Excess transfer buffer soaked the fibre pads and nitrocellulose membrane for 10 minutes. The fibre pad had nitrocellulose membrane laid on top of it, and the SDS-PAGE gel was laid on top of the nitrocellulose membrane. The whole set up was then covered with another fibre pad to make a gel sandwich. A plastic roller was used to remove any trapped air bubbles which could reduce the efficiency of transfer. Utilizing the TransBlot® Turbo Transfer System (25V, 30 min), proteins were electro-transferred onto a nitrocellulose membrane.

The voltage applied produces an electric current that is perpendicular to the gel surface, this results in the migration of the negatively charged proteins from the gel onto the nitrocellulose membrane.

3.6.6. Blocking and antibody incubation

Membranes were subsequently blocked in 5 ml of 5% BSA in Tris-buffered saline with 0.05% Tween 20 [TTBS; 150 mM NaCl, 3 mM KCl, 25 mM Tris, 0.05% Tween 20, dH_2O, pH 7.5] for 60 minutes at RT with gentle shaking preventing the non-specific binding of proteins. They were then incubated in primary antibodies (Table 4) against MBD2, DNMT3A, DNMT1, NRF2, GPx, CAT, and SOD2 and incubated for 60 minutes at RT by shaking gently and further incubated overnight (4°C). Following the overnight incubation, they were equilibrated to RT and washed with 10 ml TTBS (5 times for 10 minutes) to remove unbound primary antibody. Membranes were then probed with horseradish

peroxidase (HRP) conjugated secondary antibodies (Table 4) (anti-rabbit and or anti-mouse; 1 hr). The secondary antibody is selective to the primary antibody to which it will adhere. TTBS (10 ml) was used to wash (5 times, 10 min) off the unattached secondary antibody.

Table 4: Dilutions of antibodies

Antibody	Dilution	Catalogue number
GPX1	1:1000 in 5% BSA	#3286 (Cell Signaling Technology, Danvers, US), rabbit polyclonal
SOD2	1:1000 in 5% BSA	#13194 (Cell Signaling Technology, Danvers, US), rabbit polyclonal
CAT	1:1000 in 5% BSA	#12980 (Cell Signaling Technology, Danvers, US), rabbit polyclonal
Nrf2	1:1000 in 5% BSA	#80593 (Cell Signaling Technology, Danvers, US), rabbit polyclonal
DNMT3A	1:1000 in 5% BSA	#3598 (Cell Signaling Technology, Danvers, US), rabbit polyclonal
DNMT1	1:1000 in 5% BSA	#5032 (Cell Signaling Technology, Danvers, US), rabbit polyclonal
MBD2	1:1000 in 5% BSA	Sc-271562 (Cell signaling Technology, Danvers, US) mouse monoclonal
Anti-rabbit IgG	1:5000 in 5% BSA	#7074 (Cell Signaling Technology, Danvers, US), rabbit polyclonal
Anti-mouse IgG	1:5000 in 5% BSA	#7076 (Cell Signaling Technology, Danvers, US), rabbit polyclonal

β – actin	1:5000 in 5% BSA	#8457 (Cell Signaling Technology, Danvers, US), rabbit polyclonal

3.6.7. Imaging

The Clarity™ Western ECL substrate kit (catalogue no. #170-5060, Bio-Rad, Hercules, CA) consists of a hydrogen peroxide substrate and advanced luminol solution. This was used for the antigen-antibody complex signal detection using the Invitrogen iBright Imager. The HRP that is conjugated to the secondary antibody interacts with the hydrogen peroxide (H_2O_2) substrate and yield oxygen radicals. Those oxygen radicals interact with luminol resulting in that luminol breaking down into aminophthalic acid which reacts with enhancer molecules causing it to luminesce and enable visualization of bands of proteins (Figure 17). The viewing reagents were added in a 1:1 ratio preparing an aliquot of 200 µl of this mixture which was added to the nitrocellulose membrane.

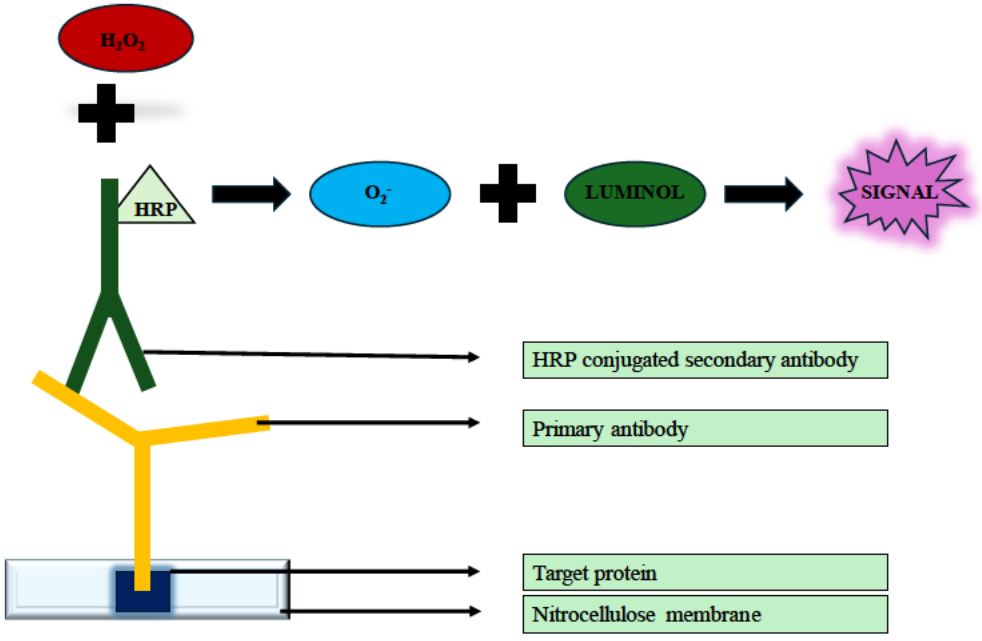

Figure 17: Antigen-antibody binding principle and detection of proteins (Prepared by author).

3.6.8. Normalization

Hydrogen peroxide (5 ml) (5%) was used to quench the membranes for 30 min at 37ºC. TTBS was used to conduct one wash (10 min, RT) and BSA (5%) was used for blocking for 60 minutes at room temperature. Membranes were then probed for β-actin (Sigma-Aldrich, MO, US; HRP-conjugated, 1:5000, 30min) (Table 2) to normalize the protein expression. The iBright Analysis Software V4.0.0 was employed to analyse protein expression and the results were presented as a fold change and relative band density (RBD). Protein expression was normalized by dividing the RBD of the protein of interest by the RBD of β-actin.

3.7. Statistical Analysis

All statistical analyses were conducted using GraphPad Prism 7. The unpaired t-test with Welch's correction assessed the significance between the control and PAT groups. A $p < 0.05$ was considered statistically significant. Tests were run in triplicate for each mouse and three times independently. The data was displayed as mean ± standard deviation.

CHAPTER 4: RESULTS

4.1. PAT Induced Oxidative Stress

4.1.1. PAT increased MDA levels

The TBARS assay quantified MDA levels, which is a biomarker of lipid peroxidation and oxidative stress. PAT significantly increased MDA levels ($p = 0.005$, control: mean ± SEM = 0.533 ± 0.049; PAT: mean ± SEM = 1.040 ± 0.137, 0.52-fold) in mice hearts (Figure 18). Results were expressed as MDA levels (µM) relative to the control and they suggest that PAT induced oxidative stress.

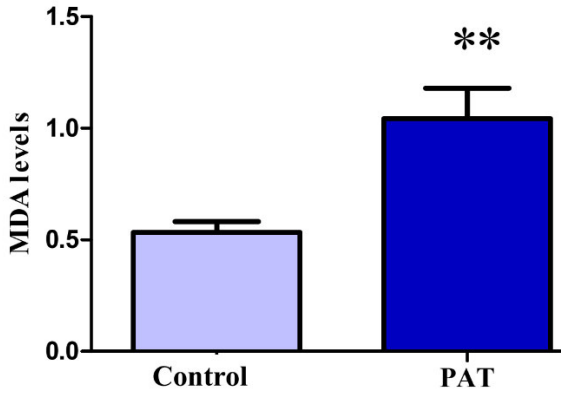

Figure 18: PAT significantly increased MDA levels in C57BL/6 mice hearts (*$p < 0.005$).

4.1.2. PAT Altered NRF2, Keap1, SOD2, CAT and GPx

Quantitative polymerase chain reaction (qPCR) showed that PAT induced oxidative stress by decreasing *keap1* expression ($p = 0.007$, control: mean ± SEM = 1.100 ± 0.022; PAT: mean ± SEM = 0.855 ± 0.077, 1.10) and significantly increasing *NRF2* ($p = 0.049$, control: mean ± SEM = 1.100 ± 0.022; PAT: mean ± SEM = 1.425 ± 0.149, 1.20-fold), *SOD2* ($p = 0.042$, control: mean ± SEM = 1.100 ± 0.022; PAT: mean ± SEM = 1.447 ± 0.126, 1.40-fold), *CAT* ($p = 0.038$, control: mean ± SEM = 1.100 ± 0.022; PAT: mean ± SEM = 1.565 ± 0.194, 0.90-fold), and *GPx* ($p = 0.028$, control: mean ± SEM = 1.100 ± 0.022; PAT: mean ± SEM = 2,056 ± 0.377, 1.20-fold) gene expressions (Figure 19). Gene expressions were normalized against the housekeeping gene, GAPDH, and expressed as relative-fold change relative to the control.

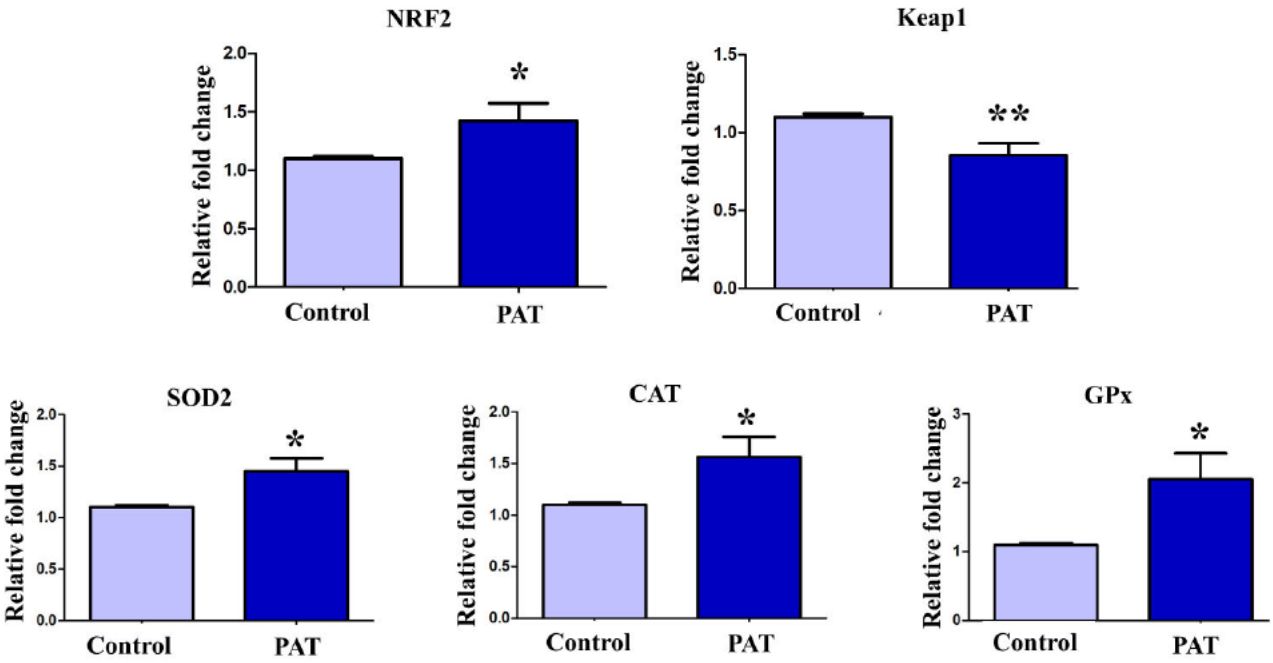

Figure 19: PAT induced oxidative stress in C57BL/6 mice hearts by significantly elevating the expression of genes *NRF2*, *SOD2*, *CAT* and *GPx* and significantly decreasing *Keap1* (*$p < 0.05$, **$p < 0.01$).

Western blot determined the effects of PAT on the protein expressions of NRF2, SOD2, and CAT. The results showed a significant increase in NRF2 ($p = 0{,}001$, control: mean ± SEM = 0.103 ± 0.036; PAT: mean ± SEM = 0.637 ± 0.137, 0.64-fold), SOD2 ($p = 0.020$, control: mean ± SEM = 1.321 ± 0.127; PAT: mean ± SEM = 2.298 ± 0.359, 2.40-fold), and CAT ($p = 0.004$, control: mean ± SEM = 0.894 ± 0.074; PAT: mean ± SEM = 1.771 ± 0.248, 1.88-fold) expression and indicates induction of oxidative stress (Figure 20).

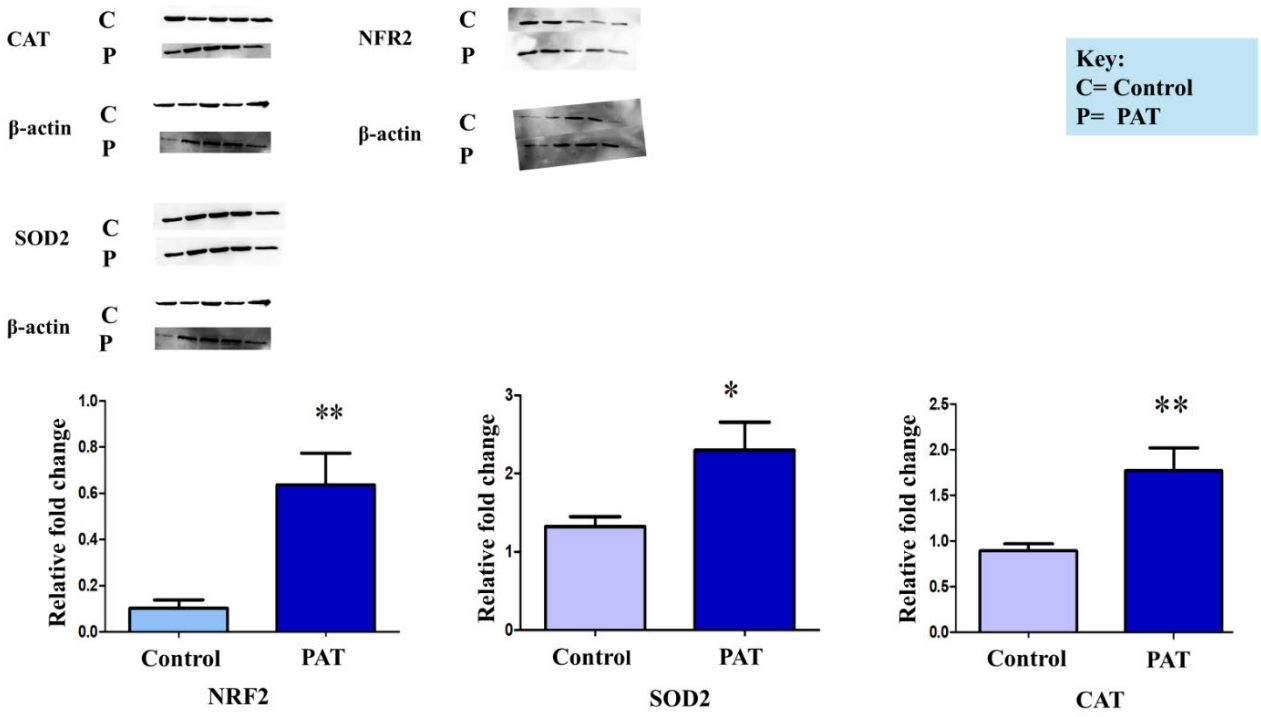

Figure 20: PAT significantly increased proteins NRF2, SOD2, and CAT in C57BL/6 mice hearts (*$p <$ 0.05, **$p < 0.001$).

4.1. PAT induced global DNA methylation

4.2.1. PAT induced global DNA hypermethylation in C57BL/6 mice hearts

ELISA quantified global DNA methylation. PAT significantly increased 5-methylcytosine levels ($p =$ 0.020, control: mean ± SEM = 0.157 ± 0.018, PAT: mean ± SEM = 0.270 ± 0.017, 1.72-fold); this suggested that PAT induced global DNA hypermethylation compared to the control samples (Figure 21).

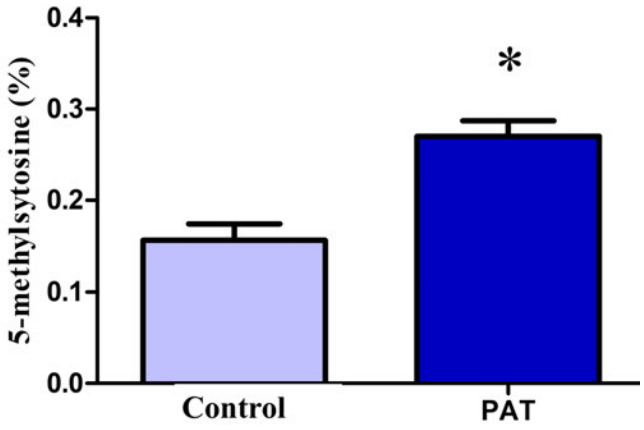

Figure 21: PAT caused global DNA hypermethylation (*$p < 0.05$) in C57BL/6 mice hearts.

4.2.2. PAT altered DNA methyltransferases

The qPCR assay assessed gene expression of DNMTs and MBD2 (Figure 22). Results showed PAT induced a significant increase in *DNMT1* ($p = 0.022$, control: mean ± SEM = 1.100 ± 0.022; PAT: mean ± SEM = 1.631 ± 0.205, 1.48-fold) and *DNMT3B* ($p = 0.041$, control: mean ± SEM = 1.100 ± 0.022; PAT: mean ± SEM = 1.766 ± 0.265, 1.62-fold), whereas it decreased *MBD2* ($p = 0.0001$, control: mean ± SEM = 1.100 ± 0.022; PAT: mean ± SEM = 0.497 ± 0.028, 0.45-fold) and *DNMT3A* ($p = 0.0001$, control: mean ± SEM = 1.100 ± 0.022; PAT: mean ± SEM = 0.453 ± 0.113, 0.41-fold) expression.

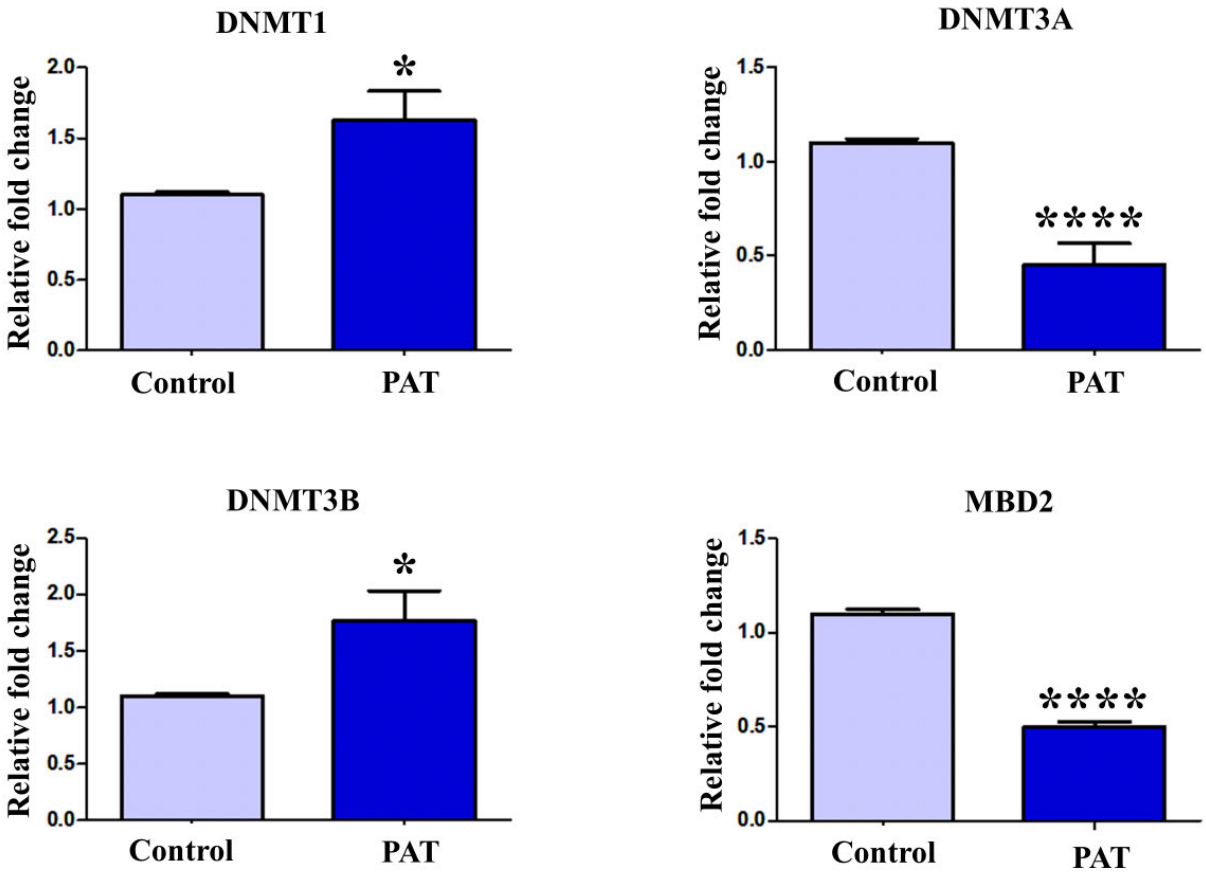

Figure 22: PAT significantly increased *DNMT1* and DNMT3B and significantly decreased *DNMT3A* and *MBD2* (*$p < 0.05$, ****$p < 0.0001$).

Western blot quantified DNMTs and MBD2 protein expression levels (Figure 23). Results showed that PAT caused DNA hypermethylation by significantly increasing DNMT1 ($p = 0.029$, control: mean ± SEM = 0.309 ± 0.075; PAT: mean ± SEM = 0.687 ± 0.099, 0.68-fold) and significantly decreasing MBD2 ($p = 0.008$, control: mean ± SEM = 1.469 ± 0.204; PAT: mean ± SEM = 0.530 ± 0.084, 0.48-fold) and DNMT3A ($p = 0.0001$, control: mean ± SEM = 1.744 ± 0.063; PAT: mean ± SEM = 0.537 ± 0.103, 0.50-fold).

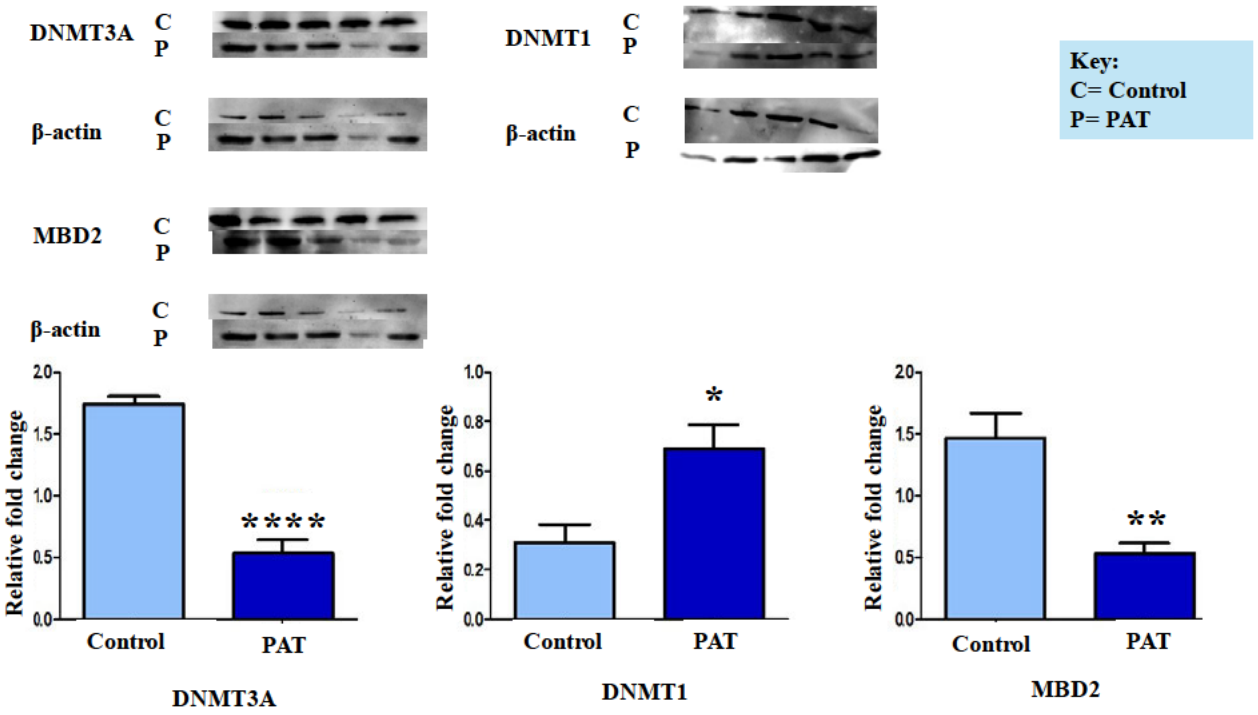

Figure 23: PAT caused DNA hypermethylation by significantly increasing DNMT1 and significantly decreasing DNMT3A and MBD2 (*$p < 0.05$, **$p < 0.01$, ****$p < 0.0001$).

CHAPTER 5: DISCUSSION

5.1. Oxidative stress

Patulin is commonly found in spoilt fruits, especially apples and apple products (Mahato *et al*., 2021). PAT consumption is toxic to both humans (*et al*Mahato *et al*., 2021, Pillay *et al*., 2023, Li *et al*., 2023) and animals (Zhang *et al*., 2024), additionally, it is toxic to plants (Li *et al*., 2024) .

Growing research has reported that PAT induces adverse health implications after consumption (Fan and Hu, 2024, Mahato *et al*., 2021). However, the mechanism by which it does this remains unclear. Some studies have shown that PAT exerts its toxicity on organs by depleting antioxidants and inducing oxidative stress (Pillay *et al*., 2020, Wei *et al*., 2020).

This study aimed to assess the mechanism by which PAT causes toxicity over 24 hours in C57BL/6 mice hearts by investigating oxidative stress and global DNA methylation.

Under physiological conditions, antioxidants balance the production of ROS from biological cell processes (Birben *et al*., 2012, Reische *et al*., 2002). Disruption of this balance by an overproduction of ROS leads to damage to organelles and biomolecules and may lead to cell death (Sies, 2020, Da Silva *et al*., 2018). Lipids are one of the affected biomolecules by ROS attack (Juan *et al*., 2021). This leads to the production of malondialdehyde (MDA) which can be measured and detect oxidative stress occurrence. The significant increase of MDA levels in the hearts of C57BL/6 mice treated with PAT compared to the control depicts the level of lipid peroxidation (Figure 18), which may be due to the overproduction of ROS induced by PAT, as research has proven that PAT induces oxidative stress (Hsu *et al*., 2023, Notardonato *et al*., 2021, Saleh and Goktepe, 2019). ROS overproduction yields oxidative stress (Wang *et al*., 2023a). These highly reactive oxygen species include superoxide, hydroxyl radical and hydrogen peroxide, which all can react with biomolecules and cause damage to them (Juan *et al*., 2021, Sesti *et al*., 2012). Studies have shown that excess ROS attacks cell membranes, causing lipid peroxidation, which also may lead to cell death (Su *et al*., 2019).

Under physiological conditions, Kelch-like ECH-associated protein 1 (Keap1) is attached to nuclear factor erythroid 2-related factor 2 (Nrf2) until there is a disturbance in the equilibrium of ROS and antioxidants (Juan *et al*., 2021, Ngo and Duennwald, 2022). In the occurrence of oxidative stress, the two dissociate and Nrf2 transcribes for antioxidant enzymes (Blaner *et al*., 2021, Sies, 2020). The expression of antioxidants can indicate the cellular oxidative stress status (Reische *et al*., 2002). In this study, Nrf2, superoxide dismutase 2 (SOD2), and catalase (CAT) all significantly increased following PAT treatment (Figure 19), which might have been because of the increased levels of MDA and oxidative stress occurrence.

Keap1 attaches to NRF2 to inactivate it and inhibit transcription of antioxidants (Song *et al*., 2021). Upon oxidative stress occurrence, this attachment breaks and Keap1 is degraded (Ulasov *et al*., 2022). The significant decrease in Keap1 levels by PAT indicates an increase in NRF2 in response to oxidative stress. This is substantiated by a significant increase in NRF2 expression by PAT. Nrf2 is a key regulator of antioxidants (Adinolfi *et al*., 2023, Liu *et al*., 2022). Elevated levels of NRF2 subsequently increased SOD2 and CAT expression (Figure 20) in the hearts of C57BL/6 mice treated with PAT. PAT also increased *GPx* expression in C57BL/6 mice hearts.

Superoxide dismutase functions to scavenge superoxide ions to oxygen and hydrogen peroxide (Zheng *et al*., 2023). Elevated levels of SOD2 gene expression indicate the presence of oxygen radicals (Zheng *et al*., 2023) and may result in the expression of their corresponding protein (Sies, 2020). Catalase functions to further convert hydrogen peroxide to water and oxygen (Baker *et al*., 2023). Increased gene function of CAT may result in its protein expression elevation too (Reische *et al*., 2002). GPx functions to reduce hydrogen peroxide to water (Pei *et al*., 2023) and its gene expression may result in protein expression (Sies, 2020)

5.2. DNA methylation

DNA methylation is an epigenetic modification that plays a role in biological processes and in disease; however, its precise need has not been fully studied (Mattei *et al*., 2022, Kobayashi *et al*., 2012). A recent study by Smith *et al*. suggests that DNA methylation is associated with gene repression, which may lead to health issues when it is unregulated (Smith *et al*., 2020). Gene repression may lead to the suppression of antioxidants and exacerbate health issues, notably, oxidative stress and its relative malignancies (Franco *et al*., 2008). PAT induced global DNA hypermethylation in C57BL/6 mice hearts by elevating DNMT3B and DNMT1 expression (Figure 22 and Figure 23). DNMT3B and DNMT3A plays a pivotal role in installing new DNA methylation patterns in previously unmethylated CpG dinucleotides (Okano *et al*., 1999). Inactivation of DNMT3A and DNMT3B has been associated with hypomethylation (Smith *et al*., 2020, Dodge *et al*., 2005). DNA hypermethylation has been associated with wound healing resistance as the genes for healing and skin repairing might be silenced (Singh *et al*., 2022, J. Dabrowski and Wojtas, 2019).

DNMT1 is associated with progressing and already established DNA methylation pattern (Kikuchi *et al*., 2022) and play an important role in maintaining DNA methylation throughout generations (Tajima *et al*., 2022). Its downregulation has been linked with hypomethylation which has been associated to adverse health implications in many studies (Novakovic *et al*., 2010, Wang *et al*., 2022). PAT upregulated DNMT1 and progressed the methylation patterns instigated by DNMT3B, leading to DNA hypermethylation. DNA hypermethylation has been associated with the progression of cancer and

enhance metastasis (Ren, 2022). In addition, DNMT1 is responsible for inactivation of the X-chromosome and gene imprinting (Okano *et al*., 1999)

DNA demethylation is as important as methylation as it ensures the amount of methylation happens in the CpG dinucleotide strands (Cheishvili *et al*., 2014). It is selective in binding to DNA that is methylated (Okano *et al*., 1999) and maintains required levels of methylation. Downregulation of MBD2 results in hypermethylation, which has previously been associated with cancer amongst many other malignancies in so many studies (Lax *et al*., 2023, Mahmood *et al*., 2024). PAT significantly decreased MBD2 and increased the C57BL/6 mice heart to susceptibility to hypermethylation.

Previous research studies have proven that PAT is involved in the induction of oxidative stress and which has led to various health issues (Liu *et al*., 2007, Zhang *et al*., 2015). This includes kidney toxicity (Han *et al*., 2021), cytotoxicity (Hsu *et al*., 2023), gastrointestinal toxicity (Qiu *et al*., 2022) and cardiotoxicity (Zhang *et al*., 2022a), which have been involved in chronic diseases such as cancer (Turkmen *et al*., 2021). Likewise, in this study, PAT was involved in inducing oxidative stress in C57BL/6 mice hearts.

Furthermore, patulin influences the progression of DNA methylation (Mazibuko *et al*., 2024). It either leads to hypermethylation or hypomethylation, which both have a role in cancer-causing processes (Tebbi, 2021, Kiruthiga and Devi, 2021). In this study, patulin induced global DNA hypermethylation in C57BL/6 mice hearts.

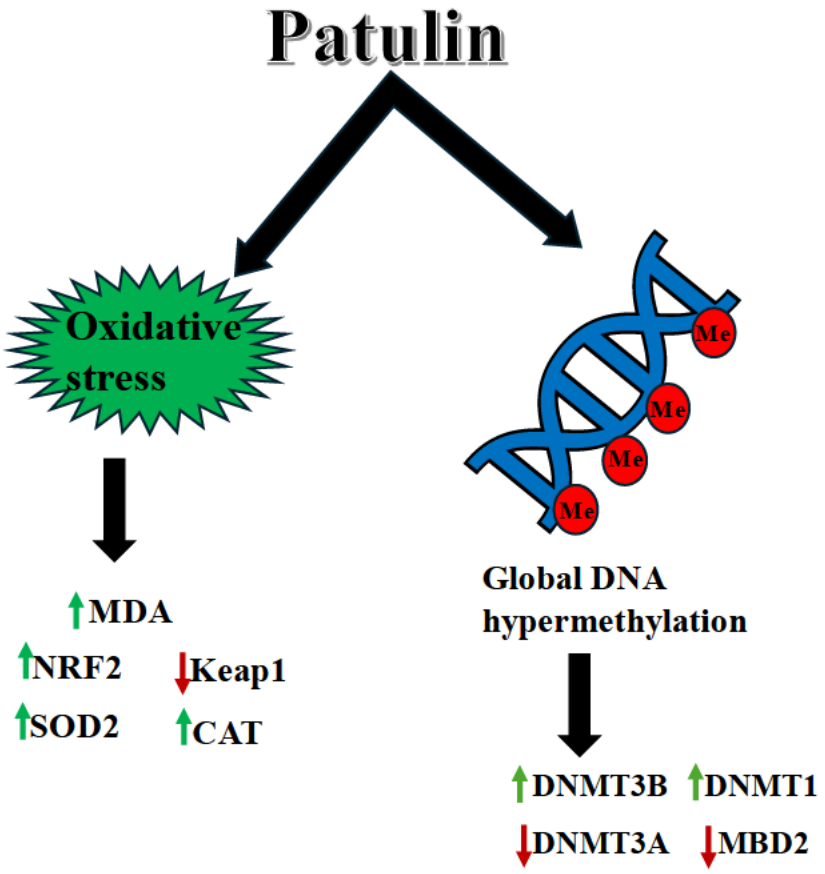

Figure 24: Mechanism of PAT induced toxicity in C57BL/6 mice hearts. PAT induces oxidative stress in C57BL/6 mice hearts, MDA levels are elevated. This trigger antioxidants activation, NRF2 levels increased and transcribed the SOD2 and CAT proteins to scavenge ROS. Keap1 levels dropped as it was deteriorated after dissociating with Nrf2. PAT also caused global DNA hypermethylation by increasing DNMT3B and DNMT1 levels, and decreasing the demethylation protein, MBD2. DNMT3A functions as DNMT3B. DNMT1 instigated new methylation pattern and DNMT3B propagated them (Prepared by author).

5. CONCLUSION

Mycotoxin contamination is a global issue that has persisted after a lot of control measures being taken, it is negatively impacting the economy and food security (Mamo *et al*., 2020, Ghazi *et al*., 2019). Patulin is commonly linked with a variety of spoilt fruits & vegetables, notably, spoilt apples (Tang *et al*., 2018, Pillay *et al*., 2020, Wei *et al*., 2020). It has gained popularity in the research field after being reported in several cases to be involved with genotoxicity, immunotoxicity, gastrointestinal toxicity, and renal toxicity (Awuchi *et al*., 2020, Zhang *et al*., 2024). A study by Zhang suggested that PAT induced cardiotoxicity, however, there hasn't been reported data up to date elucidating the mechanism by which PAT induces toxicity (Zhang *et al*., 2022a).

It is vital and recommended to understand the mechanisms by which PAT induces a variety of toxicities. This is to help reduce and avoid the level of contamination and life-threatening diseases it causes. Emphasis on these implications applies in developing countries as they are more prone to contamination and insecurity of food.

In the present study, there is an elevation of MDA levels which is a biomarker of lipid peroxidation suggesting that OS occurred. In response to relatively increasing ROS induced by PAT, there was an activation of the antioxidant response system. Nrf2 increased and transcription of OS genes and relative proteins including SOD2, and CAT were activated.

PAT induced global DNA hypermethylation by decreasing MBD2 and increasing DNMT3A.

This study was limited to a small number of mice (n = 5) per experimental group, which may have affected the variability and validity of the findings. Additionally, studies using more mice are required to verify these results. Another limitation was the short period of PAT exposure and lack of NRF2 promoter methylation data, thus future studies need to further investigate PAT under prolonged period of exposure in mice hearts and investigate the NRF2 promoter methylation. Moreover, evaluation of other mechanisms beyond oxidative stress and DNA methylation such as apoptosis, microRNA expression levels and histone modification are required.

REFERENCES

AAPOLA, U., MÄENPÄÄ, K., KAIPIA, A. & PETERSON, P. 2004. Epigenetic modifications affect Dnmt3L expression. *Biochemical Journal,* 380**,** 705-713.

ADINOLFI, S., PATINEN, T., DEEN, A. J., PITKÄNEN, S., HÄRKÖNEN, J., KANSANEN, E., KÜBLBECK, J. & LEVONEN, A.-L. 2023. The KEAP1-NRF2 pathway: Targets for therapy and role in cancer. *Redox Biology,* 63**,** 102726.

ARISTIL, J., VENTURINI, G., MADDALENA, G., TOFFOLATTI, S. L. & SPADA, A. 2020. Fungal contamination and aflatoxin content of maize, moringa and peanut foods from rural subsistence farms in South Haiti. *Journal of stored products research,* 85**,** 101550.

ASHE, A., COLOT, V. & OLDROYD, B. P. 2021. How does epigenetics influence the course of evolution? : The Royal Society.

AWUCHI, C. G. & OGUEKE, C. 2021. Mycotoxin Levels and Impacts on Chemical and Functional Properties of some Grains Sold in Owerri, Imo State, Nigeria. *Retrieved March,* 7.

AWUCHI, C. G., ONDARI, E. N., NWOZO, S., ODONGO, G. A., ESEOGHENE, I. J., TWINOMUHWEZI, H., OGBONNA, C. U., UPADHYAY, A. K., ADELEYE, A. O. & OKPALA, C. O. R. 2022. Mycotoxins' toxicological mechanisms involving humans, livestock and their associated health concerns: A review. *Toxins,* 14**,** 167.

AWUCHI, C. G., OWUAMANAM, I. C., OGUEKE, C. C. & HANNINGTON, T. 2020. The impacts of mycotoxins on the proximate composition and functional properties of grains. *Eur. Acad. Res,* 8**,** 1024-1071.

BAKER, A., LIN, C.-C., LETT, C., KARPINSKA, B., WRIGHT, M. H. & FOYER, C. H. 2023. Catalase: A critical node in the regulation of cell fate. *Free Radical Biology and Medicine,* 199**,** 56-66.

BAYR, H. 2005. Reactive oxygen species. *Critical care medicine,* 33**,** S498-S501.

BIRBEN, E., SAHINER, U. M., SACKESEN, C., ERZURUM, S. & KALAYCI, O. 2012. Oxidative stress and antioxidant defense. *World allergy organization journal,* 5**,** 9-19.

BLANER, W. S., SHMARAKOV, I. O. & TRABER, M. G. 2021. Vitamin A and vitamin E: will the real antioxidant please stand up? *Annual review of nutrition,* 41**,** 105-131.

CHEISHVILI, D., CHIK, F., LI, C. C., BHATTACHARYA, B., SUDERMAN, M., ARAKELIAN, A., HALLETT, M., RABBANI, S. A. & SZYF, M. 2014. Synergistic effects of combined DNA methyltransferase inhibition and MBD2 depletion on breast cancer cells; MBD2 depletion blocks 5-aza-2′-deoxycytidine-triggered invasiveness. *Carcinogenesis,* 35**,** 2436-2446.

CHEN, J. F. & YAN, Q. 2021. The roles of epigenetics in cancer progression and metastasis. *Biochemical Journal,* 478**,** 3373-3393.

CHENG, X. & BLUMENTHAL, R. M. 2008. Mammalian DNA methyltransferases: a structural perspective. *Structure,* 16**,** 341-350.

COELHO, F. S., SANGI, S., MORAES, J. L., DA SILVA SANTOS, W., GAMOSA, E. A., FERNANDES, K. V. S. & GRATIVOL, C. 2022. Methyl-CpG binding proteins (MBD) family evolution and conservation in plants. *Gene,* 824**,** 146404.

COMMISSION, E. 2003. Commission regulation (EC) No. 1425/2003 of 11 August 2003 amending regulation (EC) No. 466/2001 as regards patulin. *Off J Eur Union,* 203**,** 1-3.

DA SILVA, E., BRACARENSE, A. & OSWALD, I. P. 2018. Mycotoxins and oxidative stress: where are we? *World Mycotoxin Journal,* 11**,** 113-134.

DAI, Y., HUANG, K., ZHANG, B., ZHU, L. & XU, W. 2017. Aflatoxin B1-induced epigenetic alterations: An overview. *Food and Chemical Toxicology,* 109**,** 683-689.

DAVALOS, V. & ESTELLER, M. 2023. Cancer epigenetics in clinical practice. *CA: a cancer journal for clinicians,* 73**,** 376-424.

DE LEON, J. A. D. & BORGES, C. R. 2020. Evaluation of oxidative stress in biological samples using the thiobarbituric acid reactive substances assay. *Journal of visualized experiments: JoVE***,** 10.3791/61122.

DEL CASTILLO FALCONI, V. M., TORRES-ARCIGA, K., MATUS-ORTEGA, G., DÍAZ-CHÁVEZ, J. & HERRERA, L. A. 2022. DNA methyltransferases: from evolution to clinical applications. *International journal of molecular sciences,* 23**,** 8994.

DODGE, J. E., OKANO, M., DICK, F., TSUJIMOTO, N., CHEN, T., WANG, S., UEDA, Y., DYSON, N. & LI, E. 2005. Inactivation of Dnmt3b in mouse embryonic fibroblasts results in DNA hypomethylation, chromosomal instability, and spontaneous immortalization. *Journal of Biological Chemistry,* 280**,** 17986-17991.

DU, Q., LUU, P.-L., STIRZAKER, C. & CLARK, S. J. 2015. Methyl-CpG-binding domain proteins: readers of the epigenome. *Epigenomics,* 7**,** 1051-1073.

EL-SAYED, R. A., JEBUR, A. B., KANG, W. & EL-DEMERDASH, F. M. 2022. An overview on the major mycotoxins in food products: Characteristics, toxicity, and analysis. *Journal of Future Foods,* 2**,** 91-102.

EMPERLE, M., BANGALORE, D. M., ADAM, S., KUNERT, S., HEIL, H. S., HEINZE, K. G., BASHTRYKOV, P., TESSMER, I. & JELTSCH, A. 2021. Structural and biochemical insight into the mechanism of dual CpG site binding and methylation by the DNMT3A DNA methyltransferase. *Nucleic acids research,* 49**,** 8294-8308.

ESKOLA, M., KOS, G., ELLIOTT, C. T., HAJŠLOVÁ, J., MAYAR, S. & KRSKA, R. 2020. Worldwide contamination of food-crops with mycotoxins: Validity of the widely cited 'FAO estimate'of 25%. *Critical reviews in food science and nutrition,* 60**,** 2773-2789.

ESLAMI, A. & LUJAN, J. 2010. Western blotting: sample preparation to detection. *Journal of visualized experiments: JoVE***,** 2359.

FAN, L. & HU, H. 2024. Involvement of multiple forms of cell death in patulin-induced toxicities. *Toxicon***,** 107768.

FEEZOR, R. J., BAKER, H. V., MINDRINOS, M., HAYDEN, D., TANNAHILL, C. L., BROWNSTEIN, B. H., FAY, A., MACMILLAN, S., LARAMIE, J. & XIAO, W. 2004. Whole blood and leukocyte RNA isolation for gene expression analyses. *Physiological genomics,* 19**,** 247-254.

FENG, Y.-Q., ZHAO, A.-H., WANG, J.-J., TIAN, Y., YAN, Z.-H., DRI, M., SHEN, W., DE FELICI, M. & LI, L. 2022. Oxidative stress as a plausible mechanism for zearalenone to induce genome toxicity. *Gene,* 829**,** 146511.

FERNÁNDEZ-CRUZ, M. L., MANSILLA, M. L. & TADEO, J. L. 2010. Mycotoxins in fruits and their processed products: Analysis, occurrence and health implications. *Journal of advanced research,* 1**,** 113-122.

FRANCO, R., SCHONEVELD, O., GEORGAKILAS, A. G. & PANAYIOTIDIS, M. I. 2008. Oxidative stress, DNA methylation and carcinogenesis. *Cancer letters,* 266**,** 6-11.

FURIAN, A. F., FIGHERA, M. R., ROYES, L. F. F. & OLIVEIRA, M. S. 2022. Recent advances in assessing the effects of mycotoxins using animal models. *Current Opinion in Food Science,* 47**,** 100874.

GARCÍA-GUEDE, Á., VERA, O. & IBÁÑEZ-DE-CACERES, I. 2020. When oxidative stress meets epigenetics: implications in cancer development. *Antioxidants,* 9**,** 468.

GHANI, M. A., BARRIL, C., BEDGOOD JR, D. R. & PRENZLER, P. D. 2017. Measurement of antioxidant activity with the thiobarbituric acid reactive substances assay. *Food chemistry,* 230**,** 195-207.

GHAZI, T., NAGIAH, S., NAIDOO, P. & CHUTURGOON, A. A. 2019. Fusaric acid-induced promoter methylation of DNA methyltransferases triggers DNA hypomethylation in human hepatocellular carcinoma (HepG2) cells. *Epigenetics,* 14**,** 804-817.

HAMAD, G. M., MEHANY, T., SIMAL-GANDARA, J., ABOU-ALELLA, S., ESUA, O. J., ABDEL-WAHHAB, M. A. & HAFEZ, E. E. 2023. A review of recent innovative strategies for controlling mycotoxins in foods. *Food Control,* 144**,** 109350.

HAN, J., JIN, C., ZHONG, Y., ZHU, J., LIU, Q., SUN, D., FENG, J., XIA, X. & PENG, X. 2021. Involvement of NADPH oxidase in patulin-induced oxidative damage and cytotoxicity in HEK293 cells. *Food and Chemical Toxicology,* 150**,** 112055.

HANDY, D. E., CASTRO, R. & LOSCALZO, J. 2011. Epigenetic modifications: basic mechanisms and role in cardiovascular disease. *Circulation,* 123**,** 2145-2156.

HAYES, J. D., DINKOVA-KOSTOVA, A. T. & TEW, K. D. 2020. Oxidative stress in cancer. *Cancer cell,* 38**,** 167-197.

HE, F. 2011. BCA (bicinchoninic acid) protein assay. *Bio-protocol***,** e44-e44.

HENDRICH, B., GUY, J., RAMSAHOYE, B., WILSON, V. A. & BIRD, A. 2001. Closely related proteins MBD2 and MBD3 play distinctive but interacting roles in mouse development. *Genes & development,* 15**,** 710-723.
HNASKO, T. S. & HNASKO, R. M. 2015. The western blot. *ELISA: Methods and Protocols***,** 87-96.
HSU, S.-S., LIN, Y.-S., CHIO, L.-M. & LIANG, W.-Z. 2023. Evaluation of the mycotoxin patulin on cytotoxicity and oxidative stress in human glioblastoma cells and investigation of protective effect of the antioxidant N-acetylcysteine (NAC). *Toxicon,* 221**,** 106957.
HUANG, H.-C., NGUYEN, T. & PICKETT, C. B. 2002. Phosphorylation of Nrf2 at Ser-40 by protein kinase C regulates antioxidant response element-mediated transcription. *Journal of Biological Chemistry,* 277**,** 42769-42774.
HUNTER, S. E., JUNG, D., DI GIULIO, R. T. & MEYER, J. N. 2010. The QPCR assay for analysis of mitochondrial DNA damage, repair, and relative copy number. *Methods,* 51**,** 444-451.
HUSSAIN, S., ASI, M. R., IQBAL, M., AKHTAR, M., IMRAN, M. & ARIÑO, A. 2020. Surveillance of patulin in apple, grapes, juices and value-added products for sale in Pakistan. *Foods,* 9**,** 1744.
J. DABROWSKI, M. & WOJTAS, B. 2019. Global DNA methylation patterns in human gliomas and their interplay with other epigenetic modifications. *International journal of molecular sciences,* 20**,** 3478.
JACKSON, L. & DOMBRINK-KURTZMAN, M. A. 2005. Patulin. *Microbiology of fruits and vegetables***,** 297-328.
JANIK, E., NIEMCEWICZ, M., CEREMUGA, M., STELA, M., SALUK-BIJAK, J., SIADKOWSKI, A. & BIJAK, M. 2020. Molecular aspects of mycotoxins—A serious problem for human health. *International journal of molecular sciences,* 21**,** 8187.
JELTSCH, A. & JURKOWSKA, R. Z. 2016. Allosteric control of mammalian DNA methyltransferases–a new regulatory paradigm. *Nucleic acids research,* 44**,** 8556-8575.
JONES, R., WIJESINGHE, S., WILSON, C., HALSALL, J., LILOGLOU, T. & KANHERE, A. 2021. A long intergenic non-coding RNA regulates nuclear localization of DNA methyl transferase-1. *Iscience,* 24.
JUAN, C. A., PÉREZ DE LA LASTRA, J. M., PLOU, F. J. & PÉREZ-LEBEÑA, E. 2021. The chemistry of reactive oxygen species (ROS) revisited: outlining their role in biological macromolecules (DNA, lipids and proteins) and induced pathologies. *International journal of molecular sciences,* 22**,** 4642.
KADER, A. & LIU, H. 1997. Interference of anthracycline derivatives with measurement of proteins with BCA. *Clinical chemistry,* 43**,** 2201-2202.
KHODAEI, D., JAVANMARDI, F. & KHANEGHAH, A. M. 2021. The global overview of the occurrence of mycotoxins in cereals: A three-year survey. *Current Opinion in Food Science,* 39**,** 36-42.
KIKUCHI, A., ONODA, H., YAMAGUCHI, K., KORI, S., MATSUZAWA, S., CHIBA, Y., TANIMOTO, S., YOSHIMI, S., SATO, H. & YAMAGATA, A. 2022. Structural basis for activation of DNMT1. *Nature Communications,* 13**,** 7130.
KIM, B. 2017. Western blot techniques. *Molecular profiling: Methods and protocols***,** 133-139.
KIM, J.-H. 2021. Multifaceted chromatin structure and transcription changes in plant stress response. *International Journal of Molecular Sciences,* 22**,** 2013.
KIRUTHIGA, C. & DEVI, K. P. 2021. Mechanisms Involved in Carcinogenesis. *Nutraceuticals and Cancer Signaling: Clinical Aspects and Mode of Action***,** 11-36.
KLICH, M., CARY, J., BELTZ, S. & BENNETT, C. 2003. Phylogenetic and morphological analysis of Aspergillus ochraceoroseus. *Mycologia,* 95**,** 1252-1260.
KOBAYASHI, H., SAKURAI, T., IMAI, M., TAKAHASHI, N., FUKUDA, A., YAYOI, O., SATO, S., NAKABAYASHI, K., HATA, K. & SOTOMARU, Y. 2012. Contribution of intragenic DNA methylation in mouse gametic DNA methylomes to establish oocyte-specific heritable marks. *PLoS genetics,* 8**,** e1002440.
KOHN, H. I. & LIVERSEDGE, M. 1944. On a new aerobic metabolite whose production by brain is inhibited by apomorphine, emetine, ergotamine, epinephrine, and menadione. *Journal of Pharmacology and Experimental Therapeutics,* 82**,** 292-300.

KOROVESIS, D., RUBIO-TOMÁS, T. & TAVERNARAKIS, N. 2023. Oxidative stress in age-related neurodegenerative diseases: An overview of recent tools and findings. *Antioxidants,* 12**,** 131.
KOWLURU, R. A. 2023. Cross talks between oxidative stress, inflammation and epigenetics in diabetic retinopathy. *Cells,* 12**,** 300.
KUBO, N., UEHARA, R., UEMURA, S., OHISHI, H., SHIRANE, K. & SASAKI, H. 2024. Combined and differential roles of ADD domains of DNMT3A and DNMT3L on DNA methylation landscapes in mouse germ cells. *Nature communications,* 15**,** 3266.
LAX, E., DO CARMO, S., ENUKA, Y., SAPOZHNIKOV, D. M., WELIKOVITCH, L. A., MAHMOOD, N., RABBANI, S. A., WANG, L., BRITT, J. P. & HANCOCK, W. W. 2023. Methyl-CpG binding domain 2 (Mbd2) is an epigenetic regulator of autism-risk genes and cognition. *Translational Psychiatry,* 13**,** 259.
LI, H., WU, W., SHEN, X., ZHANG, W., WANG, K. & WANG, Y. 2024. Wuyiencin reduces the virulence and patulin production of Penicillium expansum by interfering with its membrane integrity and the patulin synthesis pathway. *Postharvest Biology and Technology,* 212**,** 112857.
LI, L., HE, Z., SHI, Y., SUN, H., YUAN, B., CAI, J., CHEN, J. & LONG, M. 2023. Role of epigenetics in mycotoxin toxicity: A review. *Environmental Toxicology and Pharmacology,* 100**,** 104154.
LI, Y. 2021. Modern epigenetics methods in biological research. *Methods,* 187**,** 104-113.
LIANG, F., ZHANG, H., GAO, H., CHENG, D., ZHANG, N., DU, J., YUE, J., DU, P., ZHAO, B. & YIN, L. 2021. Liquiritigenin decreases tumorigenesis by inhibiting DNMT activity and increasing BRCA1 transcriptional activity in triple-negative breast cancer. *Experimental Biology and Medicine,* 246**,** 459-466.
LIU, B.-H., WU, T.-S., YU, F.-Y. & SU, C.-C. 2007. Induction of oxidative stress response by the mycotoxin patulin in mammalian cells. *Toxicological Sciences,* 95**,** 340-347.
LIU, J., LIU, Q., HAN, J., FENG, J., GUO, T., LI, Z., MIN, F., JIN, R. & PENG, X. 2021a. N-Acetylcysteine inhibits patulin-induced apoptosis by affecting ROS-mediated oxidative damage pathway. *Toxins,* 13**,** 595.
LIU, R., DING, Y., LI, W., LI, S., LI, X., ZHAO, D., ZHANG, Y., WEI, G. & ZHANG, X. 2023a. Protective role of curcumin on broiler liver by modulating aflatoxin B1-induced DNA methylation and CYPs expression. *Ecotoxicology and Environmental Safety,* 260**,** 115086.
LIU, S., PI, J. & ZHANG, Q. 2022. Signal amplification in the KEAP1-NRF2-ARE antioxidant response pathway. *Redox biology,* 54**,** 102389.
LIU, T., LV, Y.-F., ZHAO, J.-L., YOU, Q.-D. & JIANG, Z.-Y. 2021b. Regulation of Nrf2 by phosphorylation: Consequences for biological function and therapeutic implications. *Free Radical Biology and Medicine,* 168**,** 129-141.
LIU, Z.-Y., SONG, K., TU, B., LIN, L.-C., SUN, H., ZHOU, Y., LI, R., SHI, Y., YANG, J.-J. & ZHANG, Y. 2023b. Crosstalk between oxidative stress and epigenetic marks: New roles and therapeutic implications in cardiac fibrosis. *Redox Biology***,** 102820.
LOSCALZO, J. & HANDY, D. E. 2014. Epigenetic modifications: basic mechanisms and role in cardiovascular disease (2013 Grover Conference series). *Pulmonary circulation,* 4**,** 169-174.
LU, Y., CHAN, Y.-T., TAN, H.-Y., LI, S., WANG, N. & FENG, Y. 2020. Epigenetic regulation in human cancer: the potential role of epi-drug in cancer therapy. *Molecular cancer,* 19**,** 1-16.
LUCIANO-ROSARIO, D., KELLER, N. P. & JURICK, W. M. 2020. Penicillium expansum: biology, omics, and management tools for a global postharvest pathogen causing blue mould of pome fruit. *Molecular Plant Pathology,* 21**,** 1391-1404.
LUO, S., DU, H., KEBEDE, H., LIU, Y. & XING, F. 2021. Contamination status of major mycotoxins in agricultural product and food stuff in Europe. *Food Control,* 127**,** 108120.
LYAGIN, I. & EFREMENKO, E. 2019. Enzymes for detoxification of various mycotoxins: origins and mechanisms of catalytic action. *Molecules,* 24**,** 2362.
MAGDINIER, F. & WOLFFE, A. P. 2001. Selective association of the methyl-CpG binding protein MBD2 with the silent p14/p16 locus in human neoplasia. *Proceedings of the National Academy of Sciences,* 98**,** 4990-4995.

MAHATO, D. K., KAMLE, M., SHARMA, B., PANDHI, S., DEVI, S., DHAWAN, K., SELVAKUMAR, R., MISHRA, D., KUMAR, A. & ARORA, S. 2021. Patulin in food: A mycotoxin concern for human health and its management strategies. *Toxicon,* 198**,** 12-23.
MAHMOOD, N., ARAKELIAN, A., SZYF, M. & RABBANI, S. A. 2024. Methyl-CpG binding domain protein 2 (Mbd2) drives breast cancer progression through the modulation of epithelial-to-mesenchymal transition. *Experimental & Molecular Medicine,* 56**,** 959-974.
MAHMOOD, T. & YANG, P.-C. 2012. Western blot: technique, theory, and trouble shooting. *North American journal of medical sciences,* 4**,** 429.
MAMO, F. T., ABATE, B. A., TESFAYE, K., NIE, C., WANG, G. & LIU, Y. 2020. Mycotoxins in Ethiopia: a review on prevalence, economic and health impacts. *Toxins,* 12**,** 648.
MATTEI, A. L., BAILLY, N. & MEISSNER, A. 2022. DNA methylation: a historical perspective. *Trends in Genetics,* 38**,** 676-707.
MAZIBUKO, M., GHAZI, T. & CHUTURGOON, A. 2024. Patulin alters alpha-adrenergic receptor signalling and induces epigenetic modifications in the kidneys of C57BL/6 mice. *Archives of Toxicology***,** 1-10.
MIRANDA-DUARTE, A. 2018. DNA methylation in osteoarthritis: current status and therapeutic implications. *The open rheumatology journal,* 12**,** 37.
MITACEK, R., MARKS, M. D., KERR, N., GALLAHER, D. & ISMAIL, B. P. 2023. Impact of extraction conditions and seed variety on the characteristics of pennycress (Thlaspi arvense) protein: a structure and function approach. *Journal of the American Oil Chemists' Society,* 100**,** 869-888.
MOORE, D. S. 2013. Behavioral genetics, genetics, and epigenetics. *Oxford handbook of developmental psychology,* 1**,** 91-128.
NGO, V. & DUENNWALD, M. L. 2022. Nrf2 and oxidative stress: A general overview of mechanisms and implications in human disease. *Antioxidants,* 11**,** 2345.
NGUYEN, T., NIOI, P. & PICKETT, C. B. 2009. The Nrf2-antioxidant response element signaling pathway and its activation by oxidative stress. *Journal of biological chemistry,* 284**,** 13291-13295.
NGUYEN, T., SHERRATT, P. J., HUANG, H.-C., YANG, C. S. & PICKETT, C. B. 2003a. Increased protein stability as a mechanism that enhances Nrf2-mediated transcriptional activation of the antioxidant response element: degradation of Nrf2 by the 26 S proteasome. *Journal of Biological Chemistry,* 278**,** 4536-4541.
NGUYEN, T., SHERRATT, P. J. & PICKETT, C. B. 2003b. Regulatory mechanisms controlling gene expression mediated by the antioxidant response element. *Annual review of pharmacology and toxicology,* 43**,** 233-260.
NITURE, S. K., KHATRI, R. & JAISWAL, A. K. 2014. Regulation of Nrf2—an update. *Free Radical Biology and Medicine,* 66**,** 36-44.
NOTARDONATO, I., GIANFAGNA, S., CASTORIA, R., IANIRI, G., DE CURTIS, F., RUSSO, M. V. & AVINO, P. 2021. Critical review of the analytical methods for determining the mycotoxin patulin in food matrices. *Reviews in Analytical Chemistry,* 40**,** 144-160.
NOVAKOVIC, B., WONG, N. C., SIBSON, M., NG, H.-K., MORLEY, R., MANUELPILLAI, U., DOWN, T., RAKYAN, V. K., BECK, S. & HIENDLEDER, S. 2010. DNA methylation-mediated down-regulation of DNA methyltransferase-1 (DNMT1) is coincident with, but not essential for, global hypomethylation in human placenta. *Journal of Biological Chemistry,* 285**,** 9583-9593.
OKANO, M., BELL, D. W., HABER, D. A. & LI, E. 1999. DNA methyltransferases Dnmt3a and Dnmt3b are essential for de novo methylation and mammalian development. *Cell,* 99**,** 247-257.
OZAWA, S., OJIRO, R., TANG, Q., ZOU, X., JIN, M., YOSHIDA, T. & SHIBUTANI, M. 2024. Involvement of multiple epigenetic mechanisms by altered DNA methylation from the early stage of renal carcinogenesis before proliferative lesion formation upon repeated administration of ochratoxin A. *Toxicology,* 506**,** 153875.
OZAWA, S., OJIRO, R., TANG, Q., ZOU, X., WOO, G. H., YOSHIDA, T. & SHIBUTANI, M. 2023. Identification of genes showing altered DNA methylation and gene expression in the renal

proximal tubular cells of rats treated with ochratoxin A for 13 weeks. *Journal of Applied Toxicology,* 43**,** 1533-1548.
PEI, J., PAN, X., WEI, G. & HUA, Y. 2023. Research progress of glutathione peroxidase family (GPX) in redoxidation. *Frontiers in pharmacology,* 14**,** 1147414.
PESTANA, E., BELAK, S., DIALLO, A., CROWTHER, J. R., VILJOEN, G. J., PESTANA, E. A., BELAK, S., DIALLO, A., CROWTHER, J. R. & VILJOEN, G. J. 2010. Real-time PCR–the basic principles. *Early, rapid and sensitive veterinary molecular diagnostics-real time PCR applications***,** 27-46.
PILLAY, Y., GHAZI, T., RAGHUBEER, S., NAGIAH, S. & CHUTURGOON, A. A. 2021. Patulin activates the NRF2 pathway by modulation of miR-144 expression in HEK293 cells. *Mycotoxin research,* 37**,** 97-103.
PILLAY, Y., NAGIAH, S. & CHUTURGOON, A. 2023. Patulin Alters Insulin Signaling and Metabolic Flexibility in HepG2 and HEK293 Cells. *Toxins,* 15**,** 244.
PILLAY, Y., NAGIAH, S., PHULUKDAREE, A., KRISHNAN, A. & CHUTURGOON, A. A. 2020. Patulin suppresses α1-adrenergic receptor expression in HEK293 cells. *Scientific Reports,* 10**,** 20115.
QIN, L., QIAO, C., SHEEN, V., WANG, Y. & LU, J. 2021. DNMT3L promotes neural differentiation by enhancing STAT1 and STAT3 phosphorylation independent of DNA methylation. *Progress in neurobiology,* 201**,** 102028.
QIU, Y., CHEN, X., CHEN, Z., ZENG, X., YUE, T. & YUAN, Y. 2022. Effects of selenium nanoparticles on preventing patulin-induced liver, kidney and gastrointestinal damage. *Foods,* 11**,** 749.
QUINA, A., BUSCHBECK, M. & DI CROCE, L. 2006. Chromatin structure and epigenetics. *Biochemical pharmacology,* 72**,** 1563-1569.
REEN, D. J. 1994. Enzyme-linked immunosorbent assay (ELISA). *Basic Protein and Peptide Protocols***,** 461-466.
REISCHE, D. W., LILLARD, D. A. & EITENMILLER, R. R. 2002. Antioxidants. *Food lipids.* CRC Press.
REN, Y. 2022. Regulatory mechanism and biological function of UHRF1–DNMT1-mediated DNA methylation. *Functional & Integrative Genomics,* 22**,** 1113-1126.
RICHARD, J. L. 2000. Mycotoxins-an overview. *Romer Labs' guide to mycotoxins,* 1**,** 1-48.
ROJAS, S., BARGHOUTH, P. G., KARABINIS, P. & OVIEDO, N. J. 2024. The DNA Methyltransferase DMAP1 is Required for Tissue Maintenance and Planarian Regeneration. *bioRxiv*.
ROJAS, S. A. 2023. *The DNA Methyltransferase DMAP1 is Evolutionary Conserved and Required for Tissue Maintenance in Planarians.* UC Merced.
ROTIMI, O. A., ONUZULU, C. D., DEWALD, A. L., EHLINGER, J., ADELANI, I. B., OLASEHINDE, O. E., ROTIMI, S. O. & GOODRICH, J. M. 2021. Early life exposure to aflatoxin B1 in rats: alterations in lipids, hormones, and DNA methylation among the offspring. *International Journal of Environmental Research and Public Health,* 18**,** 589.
SALEH, I. & GOKTEPE, I. 2019. The characteristics, occurrence, and toxicological effects of patulin. *Food and chemical toxicology,* 129**,** 301-311.
SCHMOLKA, N., KAREMAKER, I. D., CARDOSO DA SILVA, R., RECCHIA, D. C., SPEGG, V., BHASKARAN, J., TESKE, M., DE WAGENAAR, N. P., ALTMEYER, M. & BAUBEC, T. 2023. Dissecting the roles of MBD2 isoforms and domains in regulating NuRD complex function during cellular differentiation. *Nature Communications,* 14**,** 3848.
SESTI, F., TSITSILONIS, O. E., KOTSINAS, A. & TROUGAKOS, I. P. 2012. Oxidative stress-mediated biomolecular damage and inflammation in tumorigenesis. *In Vivo,* 26**,** 395-402.
SIES, H. 2020. Oxidative stress: Concept and some practical aspects. *Antioxidants,* 9**,** 852.
SINGH, K., RUSTAGI, Y., ABOUHASHEM, A. S., TABASUM, S., VERMA, P., HERNANDEZ, E., PAL, D., KHONA, D. K., MOHANTY, S. K. & KUMAR, M. 2022. Genome-wide DNA hypermethylation opposes healing in patients with chronic wounds by impairing epithelial-mesenchymal transition. *The Journal of clinical investigation,* 132.
SMITH, J., SEN, S., WEEKS, R. J., ECCLES, M. R. & CHATTERJEE, A. 2020. Promoter DNA hypermethylation and paradoxical gene activation. *Trends in cancer,* 6**,** 392-406.

SMITH, J. P., RALBOVSKY, N. M., LAURO, M. L., HOYT, E., GUETSCHOW, E. D., WANG, F., MCINTOSH, J. A., LIU, Z., MANGION, I. & VARIANKAVAL, N. 2022. Quantitation and speciation of residual protein within active pharmaceutical ingredients using image analysis with SDS-PAGE. *Journal of Pharmaceutical and Biomedical Analysis,* 207**,** 114393.

SMITH, Z. D., HETZEL, S. & MEISSNER, A. 2024. DNA methylation in mammalian development and disease. *Nature Reviews Genetics***,** 1-24.

SONG, M.-Y., LEE, D.-Y., CHUN, K.-S. & KIM, E.-H. 2021. The role of NRF2/KEAP1 signaling pathway in cancer metabolism. *International journal of molecular sciences,* 22**,** 4376.

STOEV, S. D. 2024. Food security, underestimated hazard of joint mycotoxin exposure and management of the risk of mycotoxin contamination. *Food Control,* 159**,** 110235.

SU, L.-J., ZHANG, J.-H., GOMEZ, H., MURUGAN, R., HONG, X., XU, D., JIANG, F. & PENG, Z.-Y. 2019. Reactive oxygen species-induced lipid peroxidation in apoptosis, autophagy, and ferroptosis. *Oxidative medicine and cellular longevity,* 2019**,** 5080843.

SUGIYAMA, K.-I., KINOSHITA, M., FURUSAWA, H., SATO, K. & HONMA, M. 2021. Epigenetic effect of the mycotoxin fumonisin B1 on DNA methylation. *Mutagenesis,* 36**,** 295-301.

SULE, R., RIVERA, G. & GOMES, A. V. 2023. Western blotting (immunoblotting): history, theory, uses, protocol and problems. *Biotechniques,* 75**,** 99-114.

SUTHIRAM, K. T., GHAZI, T., ABDUL, N. S. & CHUTURGOON, A. A. 2023. Kojic acid induces oxidative stress and anti-inflammatory effects in human hepatocellular carcinoma (HepG2) cells. Toxicon, 232, 107221.

TAGUCHI, K. & YAMAMOTO, M. 2020. The KEAP1–NRF2 system as a molecular target of cancer treatment. *Cancers,* 13**,** 46.

TAJIMA, S., SUETAKE, I., TAKESHITA, K., NAKAGAWA, A., KIMURA, H. & SONG, J. 2022. Domain structure of the Dnmt1, Dnmt3a, and Dnmt3b DNA methyltransferases. *DNA Methyltransferases-Role and Function***,** 45-68.

TANG, H., PENG, X., LI, X., MENG, X. & LIU, B. 2018. Biodegradation of mycotoxin patulin in apple juice by calcium carbonate immobilized porcine pancreatic lipase. *Food Control,* 88**,** 69-74.

TANNOUS, J., ATOUI, A., EL KHOURY, A., FRANCIS, Z., OSWALD, I. P., PUEL, O. & LTEIF, R. 2016. A study on the physicochemical parameters for P enicillium expansum growth and patulin production: effect of temperature, pH, and water activity. *Food Science & Nutrition,* 4**,** 611-622.

TEBBI, C. K. 2021. Etiology of acute leukemia: A review. *Cancers,* 13**,** 2256.

TRUONG, N., TESFAMARIAM, K., VISINTIN, L., GOESSENS, T., DE SAEGER, S., LACHAT, C. & DE BOEVRE, M. 2023. Associating multiple mycotoxin exposure and health outcomes: current statistical approaches and challenges. *World Mycotoxin Journal,* 16**,** 25-32.

TURKMEN, N. B., YUCE, H., OZEK, D. A., ASLAN, S., YASAR, S. & UNUVAR, S. 2021. Dose dependent cytotoxic activity of patulin on neuroblastoma, colon and breast cancer cell line.

ULASOV, A. V., ROSENKRANZ, A. A., GEORGIEV, G. P. & SOBOLEV, A. S. 2022. Nrf2/Keap1/ARE signaling: Towards specific regulation. *Life Sciences,* 291**,** 120111.

ÜLGER, T. G., UÇAR, A., ÇAKıROĞLU, F. P. & YILMAZ, S. 2020. Genotoxic effects of mycotoxins. *Toxicon,* 185**,** 104-113.

WANG, B., WANG, Y., ZHANG, J., HU, C., JIANG, J., LI, Y. & PENG, Z. 2023a. ROS-induced lipid peroxidation modulates cell death outcome: mechanisms behind apoptosis, autophagy, and ferroptosis. *Archives of toxicology,* 97**,** 1439-1451.

WANG, C., LEI, L., XU, Y., LI, Y., ZHANG, J., XU, Y. & SI, S. 2024. Trichostatin C synergistically interacts with DNMT inhibitor to induce antineoplastic effect via inhibition of axl in bladder and lung cancer cells. *Pharmaceuticals,* 17**,** 425.

WANG, K., NGEA, G. L. N., GODANA, E. A., SHI, Y., LANHUANG, B., ZHANG, X., ZHAO, L., YANG, Q., WANG, S. & ZHANG, H. 2023b. Recent advances in Penicillium expansum infection mechanisms and current methods in controlling P. expansum in postharvest apples. *Critical Reviews in Food Science and Nutrition,* 63**,** 2598-2611.

WANG, Y.-Y., GAO, B., YANG, Y., JIA, S.-B., MA, X.-P., ZHANG, M.-H., WANG, L.-J., MA, A.-Q. & ZHANG, Q.-N. 2022. Histone deacetylase 3 suppresses the expression of SHP-1 via deacetylation of DNMT1 to promote heart failure. *Life Sciences,* 292**,** 119552.

WEBSTER, K. E., O'BRYAN, M. K., FLETCHER, S., CREWTHER, P. E., AAPOLA, U., CRAIG, J., HARRISON, D. K., AUNG, H., PHUTIKANIT, N. & LYLE, R. 2005. Meiotic and epigenetic defects in Dnmt3L-knockout mouse spermatogenesis. *Proceedings of the National Academy of Sciences,* 102**,** 4068-4073.

WEI, C., YU, L., QIAO, N., ZHAO, J., ZHANG, H., ZHAI, Q., TIAN, F. & CHEN, W. 2020. Progress in the distribution, toxicity, control, and detoxification of patulin: A review. *Toxicon,* 184**,** 83-93.

WOOD, K. H. & ZHOU, Z. 2016. Emerging molecular and biological functions of MBD2, a reader of DNA methylation. *Frontiers in genetics,* 7**,** 93.

YIANNIKOURIS, A. & JOUANY, J.-P. 2002a. Mycotoxins in feeds and their fate in animals: a review. *Animal Research,* 51**,** 81-99.

YIANNIKOURIS, A. & JOUANY, J. 2002b. Mycotoxins in feeds for ruminants; fate and effects on animals.

YU, L., QIAO, N., ZHAO, J., ZHANG, H., TIAN, F., ZHAI, Q. & CHEN, W. 2020. Postharvest control of Penicillium expansum in fruits: A review. *Food bioscience,* 36**,** 100633.

ZHANG, B., HUANG, C., XU, D., HUANG, K., LI, Y., JIAO, L., FU, B., LI, S. & LI, Y. 2024. Patulin induces ROS-dependent cardiac cell toxicity by inducing DNA damage and activating endoplasmic reticulum stress apoptotic pathway. *Ecotoxicology and Environmental Safety,* 269**,** 115784.

ZHANG, B., LIANG, H., HUANG, K., LI, J., XU, D., HUANG, C. & LI, Y. 2022a. Cardiotoxicity of patulin was found in H9c2 cells. *Toxicon,* 207**,** 21-30.

ZHANG, B., PENG, X., LI, G., XU, Y., XIA, X. & WANG, Q. 2015. Oxidative stress is involved in Patulin induced apoptosis in HEK293 cells. *Toxicon,* 94**,** 1-7.

ZHANG, B., XU, D., SHAO, L., LIANG, H., LI, J. & HUANG, C. 2022b. Toxicity mechanism of patulin on 293 T cells and correlation analysis of Caspase family. *Toxicology Research,* 11**,** 758-764.

ZHANG, L., WANG, S., WU, G.-R., YUE, H., DONG, R., ZHANG, S., YU, Q., YANG, P., ZHAO, J. & ZHANG, H. 2023. MBD2 facilitates tumor metastasis by mitigating DDB2 expression. *Cell Death & Disease,* 14**,** 303.

ZHAO, L.-Y., SONG, J., LIU, Y., SONG, C.-X. & YI, C. 2020. Mapping the epigenetic modifications of DNA and RNA. *Protein & cell,* 11**,** 792-808.

ZHENG, M., LIU, Y., ZHANG, G., YANG, Z., XU, W. & CHEN, Q. 2023. The applications and mechanisms of superoxide dismutase in medicine, food, and cosmetics. *Antioxidants,* 12**,** 1675.

ZHOU, J., GONG, W., TU, T., ZHANG, J., XIA, X., ZHAO, L., ZHOU, X. & WANG, Y. 2023. Transcriptome analysis and functional characterization reveal that Peclg gene contributes to the virulence of Penicillium expansum on apple fruits. *Foods,* 12**,** 479.

ZHU, L., TANG, N., HANG, H., ZHOU, Y., DONG, J., YANG, Y., MAO, L., QIU, Y., FU, X. & CAO, W. 2024. Loss of Claudin-1 incurred by DNMT aberration promotes pancreatic cancer progression. *Cancer Letters,* 586**,** 216611.

ZHU, L., YUHAN, J., HUANG, K., HE, X., LIANG, Z. & XU, W. 2021. Multidimensional analysis of the epigenetic alterations in toxicities induced by mycotoxins. *Food and Chemical Toxicology,* 153**,** 112251.

ZIMMER, C. 2021. An imaging and modeling approach to characterize the structure of DNA in human cells.

APPENDIX A

Ethics Approval Letter

UNIVERSITY OF KWAZULU-NATAL
INYUVESI YAKWAZULU-NATALI

18 September 2018

Professor Anil Chuturgoon (34866)
School of Laboratory Medicine & Medical Sciences
Howard College Campus

Dear Professor Chuturgoon,

Protocol reference number: AREC/079/016
Project title: The molecular and epigenetic effects of selected mycotoxins on C57B/6 black mice

Full Approval – Renewal Application

With regards to your renewal application received on 24 August 2018. The documents submitted have been accepted by the Animal Research Ethics Committee and **FULL APPROVAL** for the protocol has been granted.

Please note: Any Veterinary and Para-Veterinary procedures must be conducted by a SAVC registered VET or SAVC authorized person.

Any alteration/s to the approved research protocol, i.e Title of Project, Location of the Study, Research Approach and Methods must be reviewed and approved through the amendment/modification prior to its implementation. In case you have further queries, please quote the above reference number.

Please note: Research data should be securely stored in the discipline/department for a period of 5 years.

The ethical clearance certificate is only valid for a period of one year from the date of issue. Renewal for the study must be applied for before 18 September 2019.

Attached to the Approval letter is a template of the Progress Report that is required at the end of the study, or when applying for Renewal (whichever comes first). An Adverse Event Reporting form has also been attached in the event of any unanticipated event involving the animals' health / wellbeing.

I take this opportunity of wishing you everything of the best with your study.

Yours faithfully

[redacted]

.....

Professor S Islam, PhD
Chair: Animal Research Ethics Committee

/ms

Cc Acting Academic Leader Research: Dr Brenda de Gama
Cc Registrar: Mr Simon Mokoena
Cc NSPCA: Ms Anita Engelbrecht
Cc BRU – Dr Linda Bester

Animal Research Ethics Committee (AREC)
Ms Mariette Snyman (Administrator)
Westville Campus, Govan Mbeki Building
Postal Address: Private Bag X54001, Durban 4000
Telephone: +27 (0) 31 260 8350 **Facsimile:** +27 (0) 31 260 4609 **Email:** animalethics@ukzn.ac.za
Website: http://research.ukzn.ac.za/Research-Ethics/Animal-Ethics.aspx

APPENDIX B

Bicinchoninic Acid (BCA) Assay

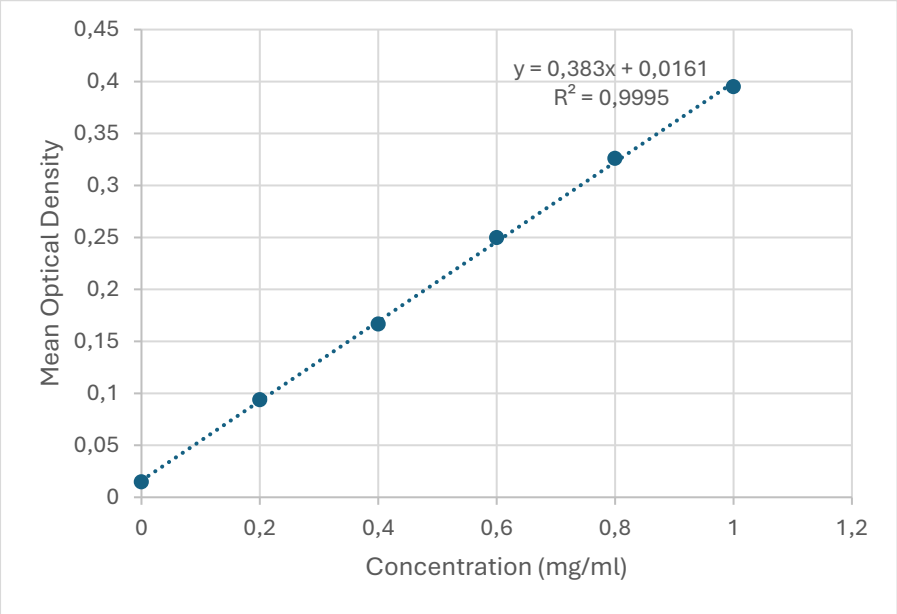

Figure 25**:** Standard curve showing known concentrations of BSA that was used to calculate the concentration of crude protein present in each sample.

APPENDIX C

Western Blot

The protein expression of GPx was investigated multiple times; however, I was unsuccessful in obtaining protein bands (Figure 28). This could have been due to multiple factors such as a defective GPx antibody. Due to limited funding, it was not possible to purchase a new GPx antibody. Moreover, due to repeating the western blot multiple times, I ran out of mice protein samples and according to the institutional ethics approval, it was not possible to sacrifice more mice to obtain more protein.

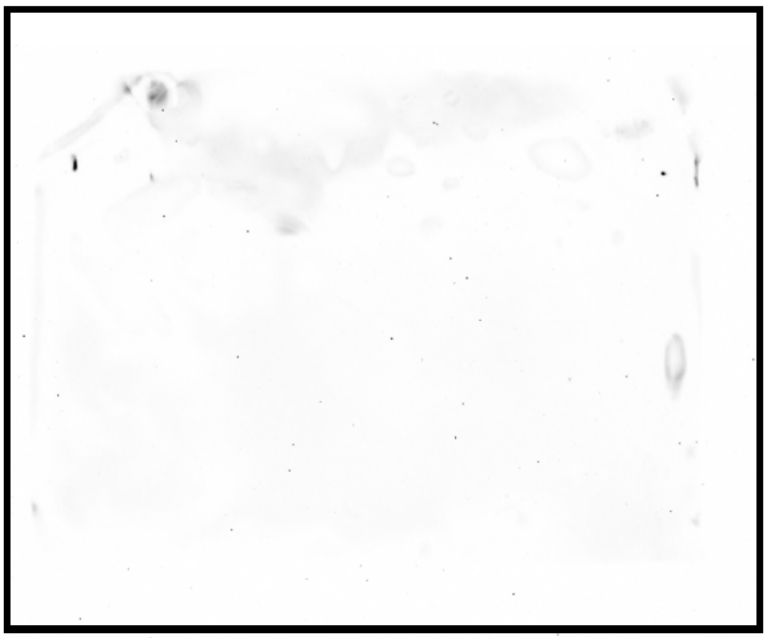

Figure 26: Western blot image for GPx.

APPENDIX D

Quantification of Global DNA Methylation

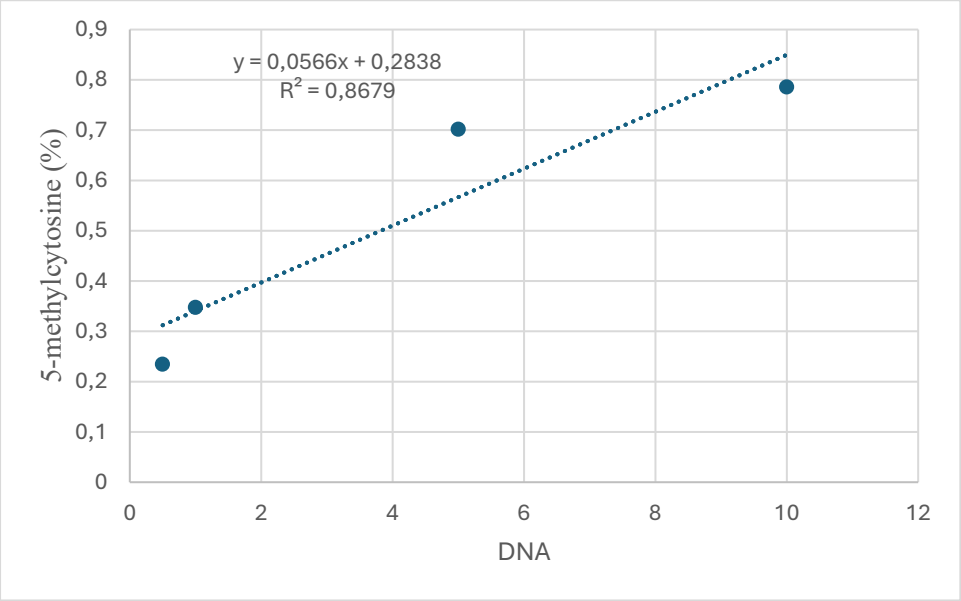

Figure 27: Standard curve used to determine the percentage of 5-methylcytosine in DNA.